Accepted Manuscript

Hydrogen sulfide donating *ent*-kaurane and spirolactone-type 6,7-*seco*-*ent*-kaurane derivatives: Design, synthesis and antiproliferative properties

Haonan Li, Xiang Gao, Xiaofang Huang, Xianhua Wang, Shengtao Xu, Takahiro Uchita, Ming Gao, Jinyi Xu, Huiming Hua, Dahong Li

PII: S0223-5234(19)30535-5

DOI: https://doi.org/10.1016/j.ejmech.2019.06.016

Reference: EJMECH 11419

To appear in: *European Journal of Medicinal Chemistry*

Received Date: 18 January 2019

Revised Date: 3 June 2019

Accepted Date: 4 June 2019

Please cite this article as: H. Li, X. Gao, X. Huang, X. Wang, S. Xu, T. Uchita, M. Gao, J. Xu, H. Hua, D. Li, Hydrogen sulfide donating *ent*-kaurane and spirolactone-type 6,7-*seco*-*ent*-kaurane derivatives: Design, synthesis and antiproliferative properties, *European Journal of Medicinal Chemistry* (2019), doi: https://doi.org/10.1016/j.ejmech.2019.06.016.

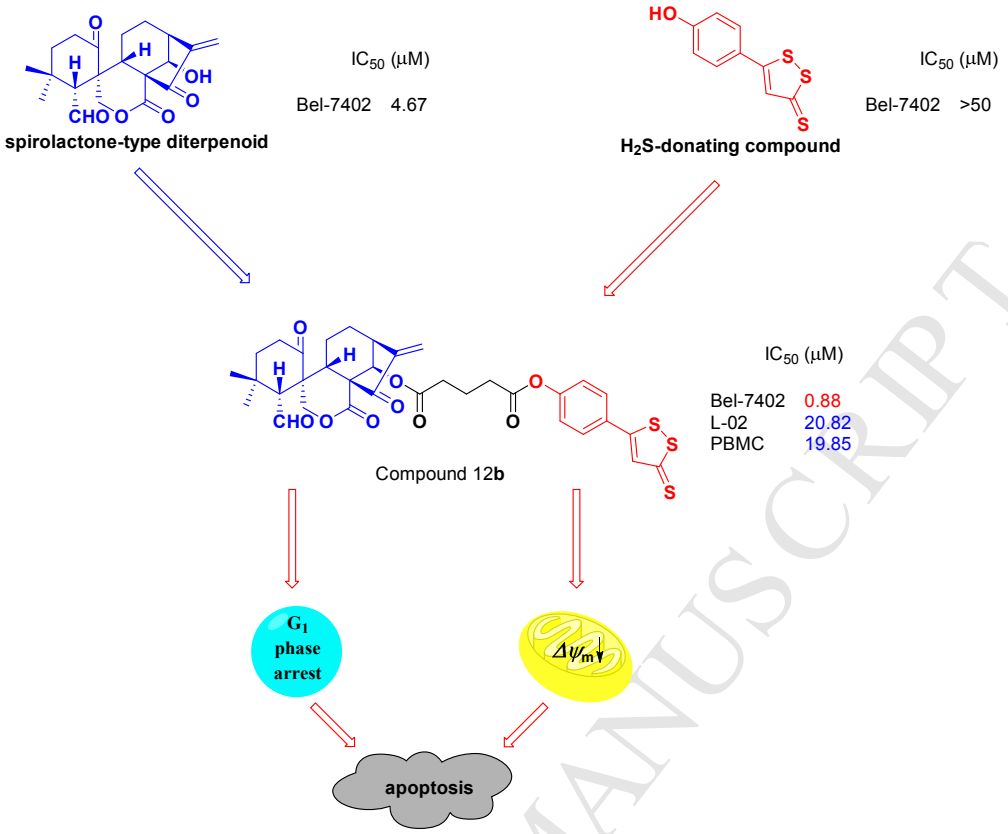

Hydrogen sulfide donating *ent*-kaurane and spirolactone-type 6,7-*seco*-*ent*-kaurane derivatives: Design, synthesis and antiproliferative properties

Haonan Li[a,1], Xiang Gao[a,1], Xiaofang Huang[a], Xianhua Wang[b], Shengtao Xu[c], Takahiro Uchita[d], Ming Gao[d], Jinyi Xu[c], Huiming Hua[a], Dahong Li[a,*]

[a]*Key Laboratory of Structure-Based Drug Design & Discovery, Ministry of Education, and School of Traditional Chinese Materia Medica, Shenyang Pharmaceutical University, 103 Wenhua Road, Shenyang 110016, P. R. China*

[b]*School of Public Health, Qingdao University, 38 Dengzhou Road, Qingdao 266021, P. R. China*

[c]*State Key Laboratory of Natural Medicines, China Pharmaceutical University, 24 Tong Jia Xiang, Nanjing 210009, P. R. China*

[d]*School of Pharmaceutical Sciences, Mukogawa Women's University, 11-68 Koshien, Nishinomiya 663-8179, Japan*

[*]Corresponding author. E-mail address: lidahong0203@163.com.

[1]These authors contributed equally to this work.

Abstract:

Motivated by our interest in hydrogen sulfide bio-chemistry and *ent*-kaurane diterpenoid chemistry, 14 hydrogen sulfide donating derivatives (**9**, **11a-c**, **12a-c**, **13**, **14**, **16a-c** and **17a-b**) of *ent*-kaurane and spirolactone-type 6,7-*seco*-*ent*-kaurane were designed and synthesized. Four human cancer cell lines (K562, Bel-7402, SGC-7901 and A549) and two normal cell lines (L-02 and PBMC) were selected for antiproliferative assay. Most derivatives showed more potent activities than the lead *ent*-kaurane oridonin. Among them, compound **12b** exhibited the most potent antiproliferative activities, with IC_{50} values of 1.01, 0.88, 4.36 and 5.21 μM against above human cancer cell lines, respectively. Further apoptosis-related mechanism study indicated that **12b** could arrest Bel-7402 cell cycle at G1 phase and induce apoptosis through mitochondria related pathway. Through western blot assay, **12b** was shown to influence the intrinsic pathway by increasing the expression of Bax, cleaved caspase-3, cytochrome *c* and cleaved PARP, meanwhile suppressing procaspase-3, Bcl-2, Bcl-xL and PARP.

***Key words*:** diterpenoid, hydrogen sulfide, antiproliferative activity, apoptosis

1. Introduction

Nature has long been an invaluable source, providing molecular skeletons for drug discovery [1]. During the 1940s to the end of 2014, almost 50% of approved anticancer small molecules were nature derived molecules [2]. The *Rabdosia*, an important and cosmopolitan genus of the Labiatae family, has aroused considerable interests due to the aboundance of *ent*-kaurane diterpenoids [3-10]. Oridonin (**1**, Fig. 1), the main active component of *Rabdosia rubescens*, has been the most extensively studied natural product of this genus [11-20]. Its structure and absolute configuration were determined in 1970 [21]. It exhibited anticancer effects on leukemia [22], pancreatic cancer [23], osteosarcoma [24], colorectal cancer [25], renal cell carcinoma [26] and diffuse large B cell lymphoma [27]. One sub-type of 6,7-*seco*-*ent*-kauranes, spirolactone-type (7,20-lactone) diterpenoids, contains multiple stereogenic centers and complex ring systems, such as trichorabdal A, maoecrystal Z, longikaurin E, sculponeatin N, maoecrystal V, sculponeatin C, laxiflorolide C and laxiflorin B (Fig. 1) [28-34]. In particular, some of them exhibited promising antiproliferative effects [35-37] with IC_{50} values of 0.21, 0.29, 0.60 and 0.80 against K562, HepG2, SW-480 and HL-60 human cancer cell lines, respectively.

Although spirolactone-type diterpenoids demonstrated sub-micromolar level antiproliferative activities, their low isolation yields from *Isodon* plants can not meet the need for further studies, which hindered their wide application as potential candidates in drug development. Moreover, the complex stereogenic centers make it quite challenging to achieve via total synthesis [38,39]. In general, through the analysis of active products [40-42], structural modification [43,44], biological evaluation [45,46] and mechanism study [47-49], the deigned derivatives would show better properties than the original forms and some of them would serve as drug candidates. In our previous work, a convenient method for the conversion from oridonin to spirolactone-type skeleton in quantitative yield was achieved by oxidation with lead tetraacetate, which could provide enough starting materials for the medicinal study of spirolactone-type derivatives [50-53].

Small molecule donors have been widely used in drug discovery [54,55]. Hydrogen sulfide (H_2S), like nitric oxide (NO) and carbon monoxide (CO), has been recognized as a gasotransmitter related to health and disease [56,57]. The generation of endogenous H_2S is caused by three important enzymes, cystathionine-γ-lyase (CSE), cystathionine-β-synthase (CBS) and 3-mercaptopyruvate sulfurtransferase (MST), with cysteine, homocysteine and cystathionine as substrate [58,59]. Besides bioactivities in vascular tone, blood pressure, ischemia-reperfusion injury, atherosclerosis, angiogenesis and neuroinflammation [60-65], recent studies elucidated that H_2S showed moderate anticancer activity by inducing cell apoptosis via EGFR/ERK/MMP-2, PI3K/Akt/mTOR and p38 MAPK/ERK1/2-COX-2 pathways [66-70]. Although H_2S plays important roles in physiology and pathology, it can not be directly used in clinical treatment due to uncontrollable dose and high toxicity. While the H_2S donors (including ADT-OH, thiobenzamide, α-thioctic acid, GYY4137, persulfides etc. Fig. 2A) could partially solve the problems which release H_2S at relative slow rates [71-74]. H_2S-releasing compounds also showed promising properties and were instrumental for the exploration of drug candidates [75-79, Fig.2B].

Based on the above, we used two *ent*-kaurane derivatives (**2**, **6**) linked with two kinds of H_2S donors (α-thioctic acid and ADT-OH) by ether bond and then converted them into corresponding spirolactone-type derivatives. The antiproliferative effects of target compounds were evaluated against chronic myelogenous leukemia K562, liver cancer Bel-7402, gastric cancer SGC-7901, lung cancer A549, human normal liver L-02 and normal peripheral blood mononuclear PBMC cell lines. Furthermore, apoptosis related mechanism of the most potent compound **12b** was also explored, including cell cycle progression, apoptotic induction, mitochondria membrane potentials decline and the expression of apoptosis-related proteins.

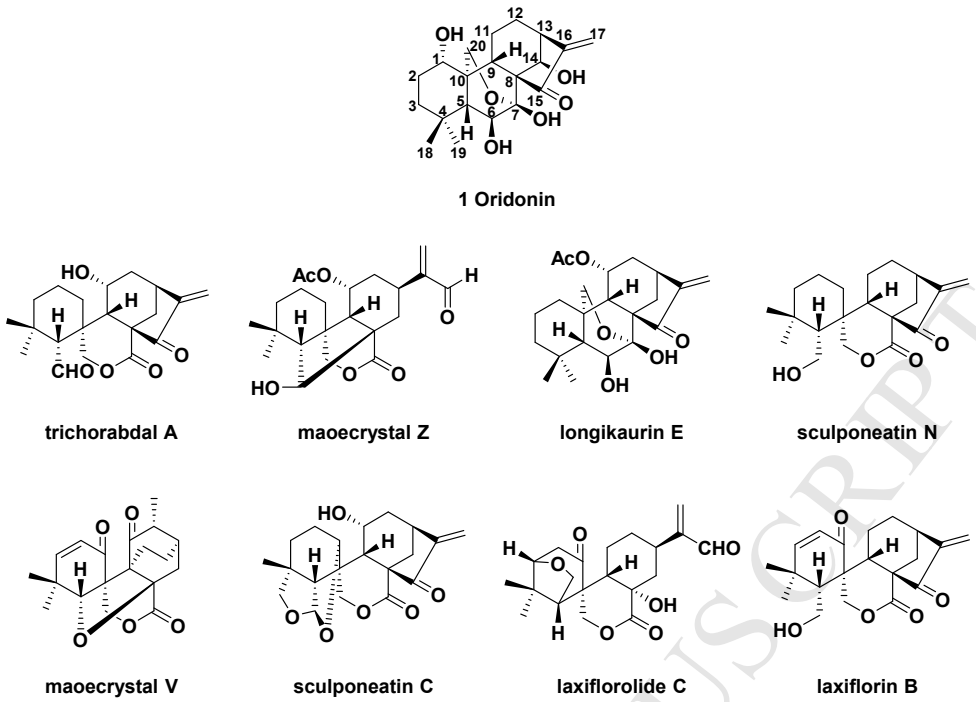

Fig. 1. The structures of oridonin and natural spirolactone-type 6,7-*seco*-*ent*-kaurane diterpenoids.

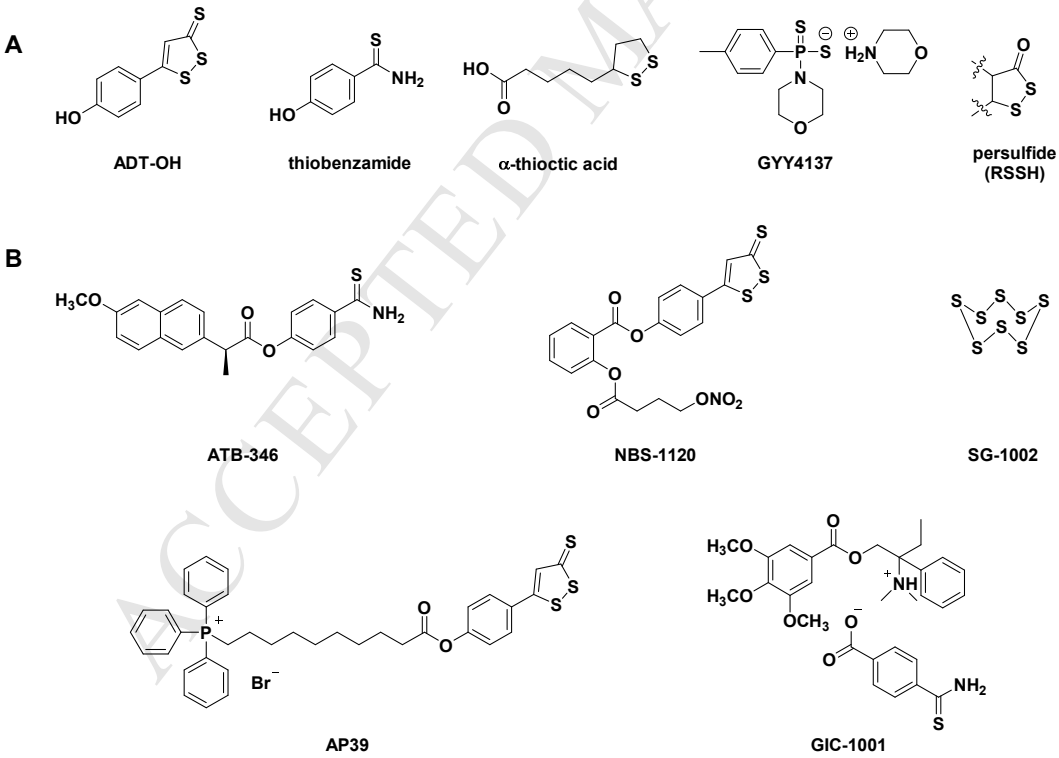

Fig. 2. The structures of selected H_2S donating molecules (A) and H_2S releasing drug candidates (B).

2. Result and discussion

2.1. Chemistry

The whole synthetic route of H_2S-releasing derivatives is outlined in Scheme 1 and Scheme 2. Intermediate **2** was obtained through addition of Jones reagent to selectively oxidize the 1-OH of **1**. Treatment of **1** with 2,2-dimethoxypropane and TsOH in anhydrous acetone afforded derivative **4**, then reaction with Ac_2O/Et_3N in DCM acquired derivative **5**. And intermediate **6** was afforded via deprotection in the presence of 10% HCl. The derivatives **3** and **7** were prepared by lead tetraacetate and sodium carbonate (Na_2CO_3) in THF. The generated **2** and **5** were reacted with corresponding anhydride under the condition of 4-dimethylaminopyridine (DMAP) and triethylamine (TEA) in DCM at room temperature, which gave derivatives **10a-c** and **15a-c** in quantitative yields. Then H_2S-releasing derivatives **8**, **11a-c**, **13** and **16a-c** were obtained via reaction of corresponding diterpenoid derivatives with ADT-OH or α-thioctic acid in the presence of DMAP and carbodiimide hydrochloride (EDCI). Finally, spirolactone-type derivatives **9**, **12a-c**, **14** and **17a-b** were achieved by oxidation using lead tetraacetate and Na_2CO_3 in THF.

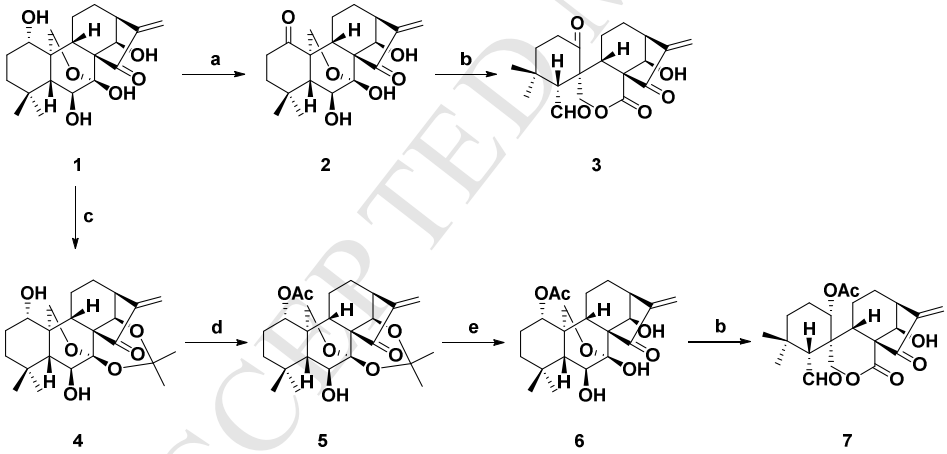

Scheme 1. The synthetic route of intermediates. Reagents and conditions: (a) Jones reagent, acetone, 0 °C, 0.5 h; (b) $Pb(OAc)_4$, Na_2CO_3, THF, rt, 2 h; (c) 2,2-dimethoxypropane, acetone, TsOH, 56 °C, 1.5 h; (d) Ac_2O, TEA, DMAP, DCM, rt, 5 h; (e) 10% HCl, THF, rt, 4 h.

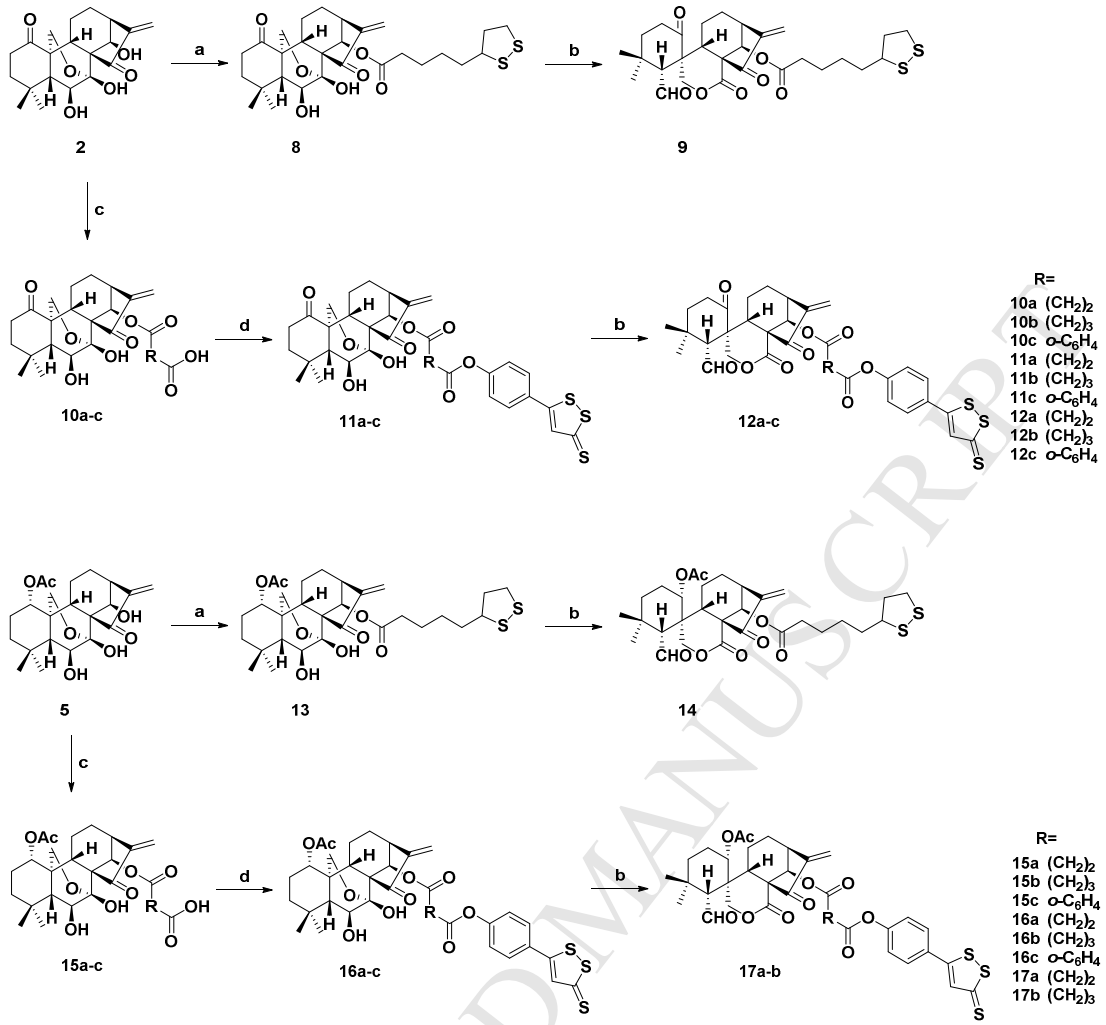

Scheme 2. Synthesis of H_2S-releasing derivatives **9**, **11a-c**, **12a-c**, **13**, **14**, **16a-c** and **17a-b**. Reagents and conditions: (a) α-thioctic acid, EDCI, DMAP, DCM, rt, 12 h; (b) $Pb(OAc)_4$, Na_2CO_3, THF, rt, 2 h; (c) corresponding anhydride, TEA, DMAP, DCM, rt, 5 h; (d) ADT-OH, EDCI, DMAP, DCM, rt, 8-12 h.

2.2. Biological evaluation

2.2.1 Antiproliferative activities and preliminary SAR

The antiproliferative activities of 14 target derivatives (**9**, **11a-c**, **12a-c**, **13**, **14**, **16a-c** and **17a-b**), lead compound oridonin (**1**), parental diterpenoids (**2**, **3**, **6** and **7**) and H_2S donors (ADT-OH and α-thioctic acid) were tested by MTT assay (5-Fu was used as positive control). Four human cancer and two normal cell lines were selected to test their cytotoxicity. As shown in Table 1, all derivatives displayed inhibitory activities against selected human cancer cell lines.

Most derivatives exhibited more potent antiproliferative activities than oridonin (IC_{50} = 4.79-18.86 μM), and even than positive control (IC_{50} = 2.33-17.59 μM). Besides promising antiproliferative activities, low cytotoxicity to normal cells was also observed, which is a key character in anticancer drug exploration. When the substitution R were alkyl groups (**11a-b**, **12a-b** and **16a-b**), their antiproliferative activities were more potent than corresponding ones with aromatic groups (**11c**, **12c** and **16c**) and improved IC_{50} values were observed with the extension of R group in Bel-7402 cells. It demonstrated that linear linker rather than benzene ring was advantageous for potency, and longer carbon bridge might contribute to superior inhibitory effects. Compounds **9**, **13** and **14** whose 14-OH directly incorporated with α-thioctic acid showed similarly antiproliferative activities to corresponding derivatives (**11a-b**, **12a-b**, **16a-b** and **17a-b**) which coupled with ADT-OH through a carbon bridge. Comparing 1-oxo *ent*-kaurane derivatives (**11a-c**) with corresponding spirolactone-type derivatives (**12a-c**), stronger antiproliferative activities were observed. But this phenomenon did not work in 1-acetylated derivatives (**16a-c** and **17a-b**). Furthermore, among spirolactone-type derivatives, 1-oxo derivatives (**12a-c**) showed more potent activities than 1-acetylated derivatives (**17a-b**). Among them, compound **12b** showed the strongest antiproliferative activities, with IC_{50} values of 1.01, 0.88, 4.36 and 5.21 μM against K562, Bel-7402, SGC-7901 and A549 human cancer cell lines, respectively. Furthermore, compound **12b** exhibited almost 24-fold less potent antiproliferative activities against L-02 (IC_{50} = 20.82 μM) and PBMC (IC_{50} = 19.85 μM) normal cell lines, demonstrating selectivity between cancer and normal cell lines. Hence, compound **12b** was selected for further mechanism study.

Table 1

Antiproliferative activities (IC_{50}^{a} μM) of 14 target derivatives, parental diterpenoids and H_2S donors against four human cancer and two normal cell lines.

Compound	K562	Bel-7402	SGC-7901	A549	L-02	PBMC
1	4.79±0.12	8.31±0.29	7.87±0.36	17.80±0.75	18.68±1.28	>50
2	4.02±0.18	3.88±0.18	16.54±0.30	9.86±0.45	23.41±1.39	>50
3	3.26±0.16	4.67±0.25	19.48±0.94	5.31±0.40	29.70±1.07	>50

6	4.92±0.24	3.59±0.18	6.45±0.37	13.47±0.53	22.36±1.25	>50
7	8.96±0.49	>50	49.84±2.51	27.44±1.52	>50	>50
9	2.59±0.22	2.56±0.19	6.43±0.37	7.92±0.77	19.85±1.37	>50
11a	3.66±0.30	3.52±0.31	12.50±0.44	9.78±0.75	>50	29.62±1.31
11b	3.84±0.28	3.04±0.23	6.59±0.26	4.38±0.17	21.02±1.36	17.23±1.05
11c	4.80±0.10	5.34±0.27	14.87±0.53	7.69±0.40	42.64±2.63	>50
12a	1.82±0.07	1.38±0.12	4.24±0.25	5.54±0.42	18.19±1.44	16.58±1.26
12b	1.01±0.07	0.88±0.05	4.36±0.20	5.21±0.25	20.82±1.28	19.85±1.37
12c	4.25±0.23	3.26±0.14	5.93±0.33	7.45±0.38	26.21±1.55	31.45±1.61
13	2.84±0.17	2.25±0.16	6.02±0.20	8.65±0.36	41.10±2.94	28.83±1.45
14	6.75±0.31	4.58±0.24	10.04±0.39	19.89±0.81	36.47±1.32	>50
16a	2.54±0.18	2.87±0.08	5.49±0.14	6.34±0.41	23.24±1.54	44.15±2.26
16b	2.02±0.06	1.94±0.12	5.36±0.28	9.76±0.48	14.70±1.14	>50
16c	11.43±0.74	7.68±0.35	12.37±0.85	16.66±0.70	>50	39.53±1.69
17a	15.26±1.08	9.73±0.52	17.95±0.76	27.53±1.21	>50	25.86±1.35
17b	3.27±0.21	4.59±0.37	7.66±0.37	14.82±1.14	>50	30.65±1.41
ADT-OH	>50	>50	>50	>50	>50	>50
α-thioctic acid	>50	>50	>50	>50	>50	>50
5-Fu	4.02±0.22	17.59±0.86	6.38±0.32	2.33±0.12	>50	>50

[a]IC_{50}: Half inhibitory concentrations measured by the MTT assay, the cells were incubated for 72 h. The values are expressed as averages ± standard deviations of three independent experiments.

2.2.2. H_2S release ability

H_2S-releasing capability of all derivatives was tested by the methylene blue (MB^+) method. As shown in Fig. 3, all derivatives could produce H_2S with a peak time around 15-20 min. It was obvious that those derivatives with α-thioctic acid (**9**, **13** and **14**) showed the highest H_2S generating ability, while releasing characteristics of the derivatives with ADT moisties were not varied significantly from each other, except for **17a** and **17b**. Interestingly, 1-oxo derivatives usually produced more H_2S (0.2-1 μM) than 1-acetylated derivatives. Two spirolactone-type

derivatives with acetyl group at C-1 (**17a-b**) were found to release the lowest H_2S, which were consistent with their tempered antiproliferative activities. Among other derivatives with ADT-OH, spirolactone-type derivatives **12a-c** showed moderate H_2S releasing ability while exhibiting superior antiproliferative activities. Furthermore, in contrast to the low antiproliferative effects, those with phthalic anhydride linker (**11c**, **12c** and **16c**) generated more H_2S. Moreover, with the increased length of R groups, stronger antiproliferative effects could be found but with a small reduction in H_2S generation.

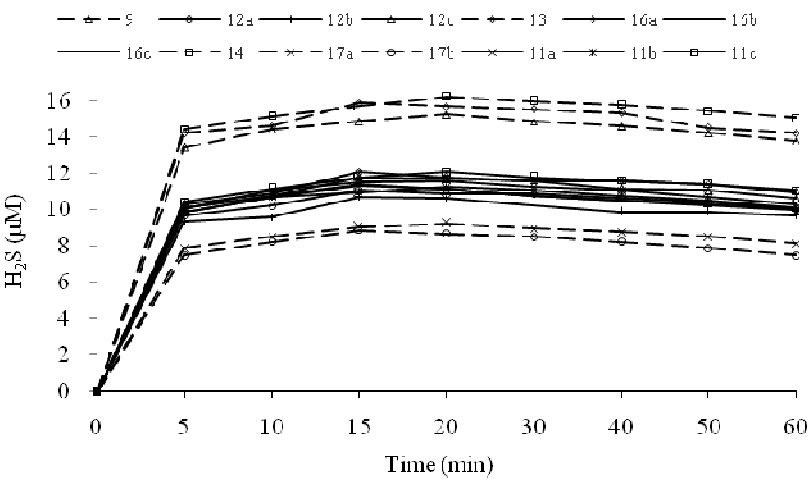

Fig. 3. H_2S-releasing ability of target compounds. The values are expressed as averages of three independent experiments.

2.2.3. Cell cycle analysis

Cell cycle is the basic process of cell life activities. An interruption of certain phase of cell cycle leads to the inhibition of cell division and suppresses tumor growth. In order to demonstrate the antiproliferative mechanism, the influence on cell cycle of **12b** was tested and DNA content of cell nuclei was measured via flow cytometry. In this assay, Bel-7402 cells were treated with different concentrations of **12b** (0, 0.45, 0.90 and 1.80 μM) for 48 h. Then stained with propidium iodide (PI) for subsequent cytometry analysis. Cells treated with DMSO were used as control. As shown in Fig. 4, after treatment with 0, 0.45, 0.90 and 1.80 μM **12b**, the percentage of Bel-7402 cells at G1 phase achieved a substantial increase from 30.95% to 37.37%, 42.30% and 49.56%,

respectively. According to the results, **12b** led to a dose-dependent accumulation of Bel-7402 cells at G1 phase.

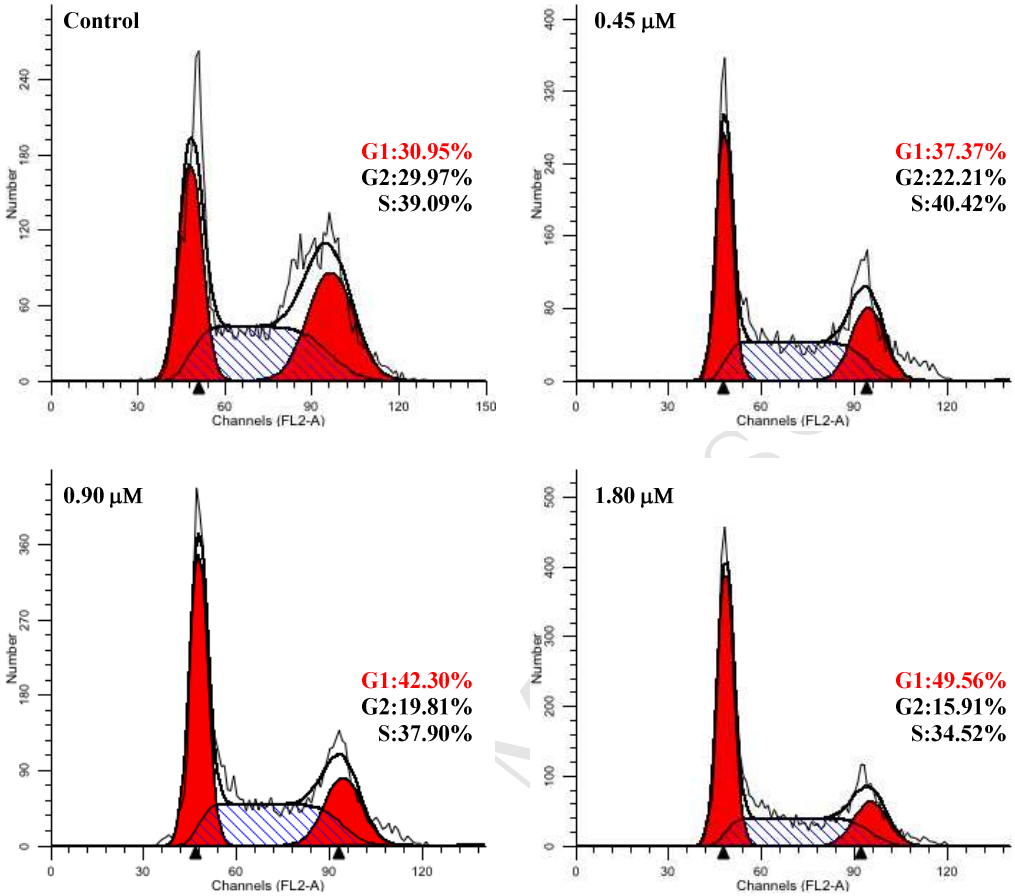

Fig. 4. Influence on Bel-7402 cell cycle of **12b**. After incubated with **12b** (0.45, 0.90 and 1.80 μM) or DMSO (control) for 48 h, Bel-7402 cells were stained with PI and then cell cycle distribution was analyzed by a flow cytometer.

2.2.4. The morphological analysis by Hoechst 33258 staining

The deviant morphological changes in chromatin, including cell shrinkage, chromatin condensation, the rupture of cell membrane and the nuclear fragmentation, indicate the occurrence of apoptosis. Hoechst 33258 staining assay was used to indicate apoptosis by fluorescence microscope [80]. As shown in Fig. 5, contrast to vehicle control, Bel-7402 cells presented bright blue chromatin shrink and nuclear fragmentation after treatment with **12b** (0.45, 0.90 and 1.80

μM). While control cells remained homogeneous nuclei with deep blue color. The Hoechst 33258 staining assay revealed that **12b** could induce apoptosis in Bel-7402 cells.

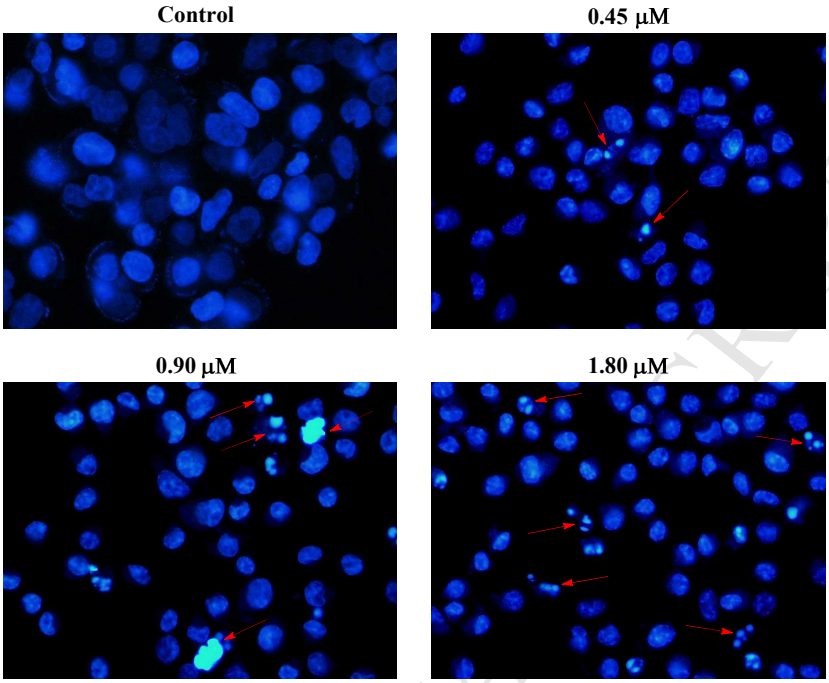

Fig. 5. Hoechst staining of **12b** treated Bel-7402 cells. After treatment with **12b** (0.45, 0.90 and 1.80 μM) or vehicle for 48 h, Bel-7402 cells were stained in blue color and probed by a fluorescent microscope.

2.2.5. Cell apoptosis assay

Apoptosis is an important biological process of programmed cell death, which maintain regular functions and activities of cells. But cancer cells could grow incessantly by suppressing apoptosis. Thus, utilizing chemical agents induced apoptosis in cancer cells is a potent therapeutic method. In order to further confirm **12b** induced apoptosis in Bel-7402 cells, an annexin V-FITC/PI binding assay was performed. Bel-7402 cells were treated with **12b** at indicated concentrations (0, 0.45, 0.90 and 1.80 μM), then the percentage of apoptotic cells was measured by a flow cytometry. As shown in Fig. 6, after incubation with **12b** for 48 h, apoptotic ratios substantially rose from 2.77% of vehicle control to 17.65%, 27.47% and 55.32% for different concentrations applied, respectively, in a dose-dependent manner. The results indicated that **12b** possessed the ability to induce apoptosis in Bel-7402 cells.

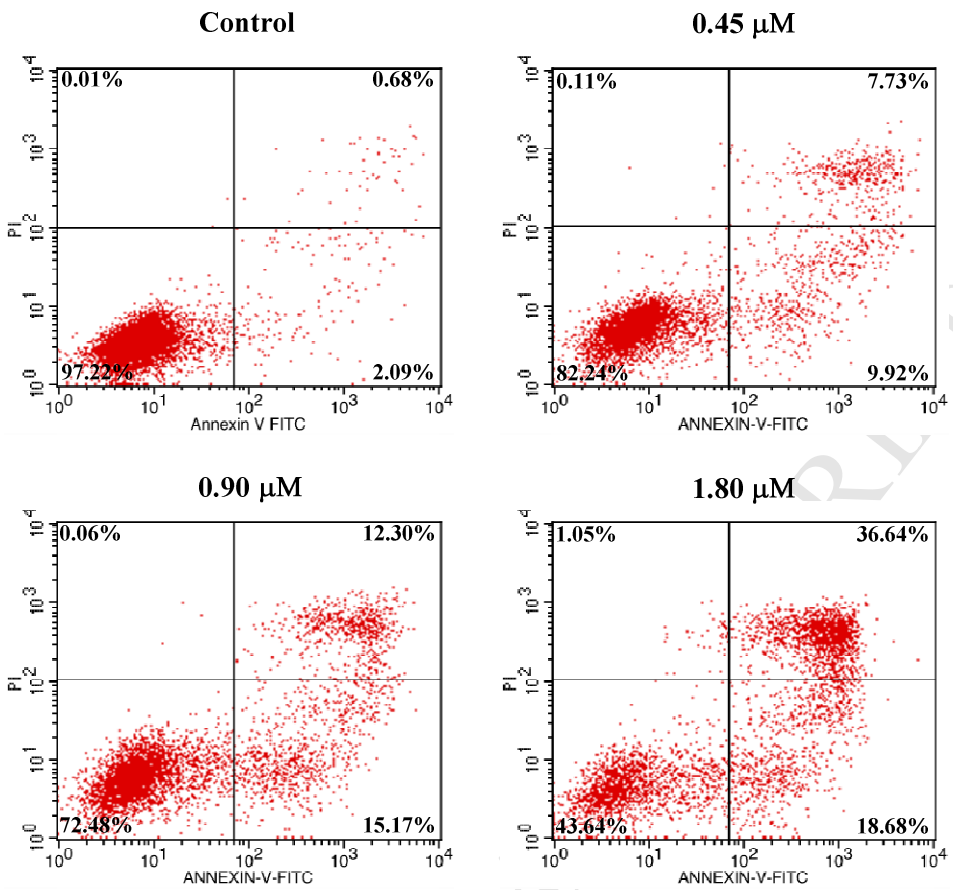

Fig. 6. Apoptosis effects of **12b** on Bel-7402 cells. Bel-7402 cells were treated with **12b** for 48 h and analyzed via an annexin V-FITC/PI binding assay.

2.2.6. Mitochondria membrane potential analysis

The maintenance of mitochondrial membrane potentials plays an important role in mitochondrial integrity and biological function. Mitochondrial changes, especially losing mitochondrial membrane potentials, were significant events taking place during drug-induced apoptosis. Additionally, endogenous H_2S was recognized to induce apoptosis by activating the intrinsic mitochondrion-mediated pathways according to recent literatures [81]. The changes of mitochondrial membrane potentials were measured via flow cytometry, in order to demonstrate the influence of **12b** on mitochondria. Bel-7402 cells were incubated for 48 h with different concentrations of **12b** (0.45, 0.90 and 1.80 μM) and vehicle control DMSO. Then cells were treated with the lipophilic cationic fluorescent probe 5,5′,6,6′-tetrachloro-1,1′,3,3′-tetraethylbenzimidazol-carbocyanine iodide (JC-1). As shown in Fig.

7, the percentage of cells with depolarized mitochondria ranged from 1.28% of control to 18.48%, 30.96% and 58.59% in a dose-dependent manner. This indicated that **12b** induced Bel-7402 cells apoptosis via mitochondria related pathway.

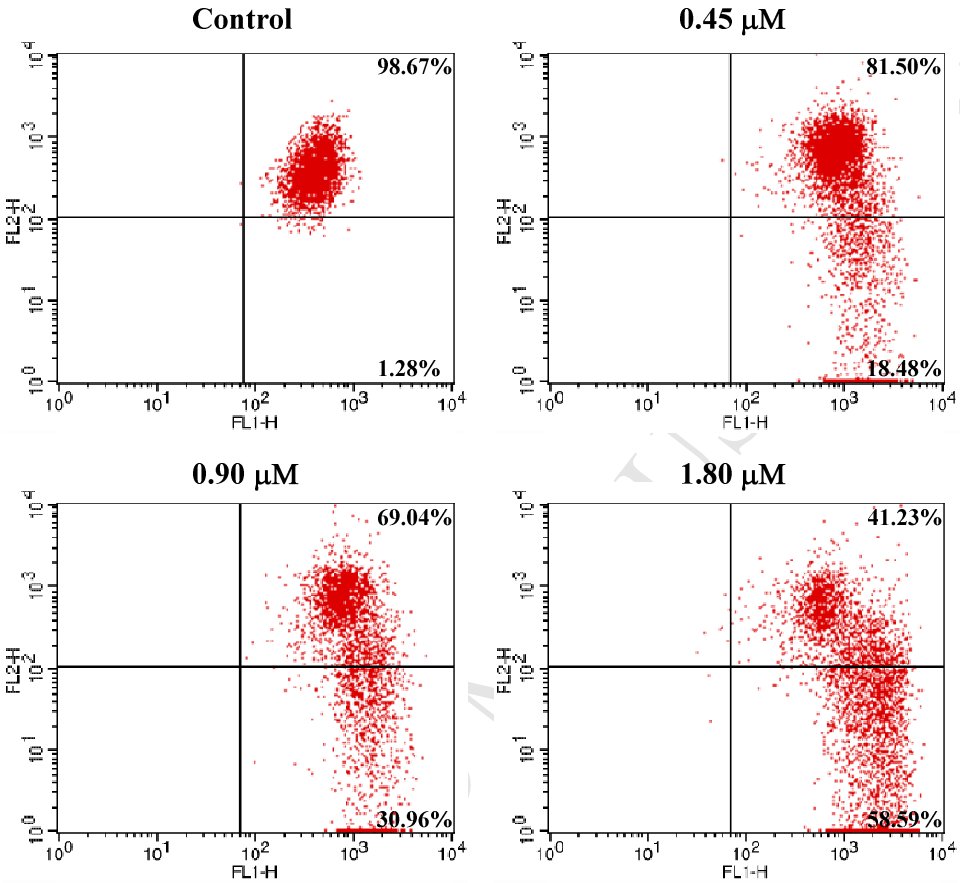

Fig. 7. Influence on mitochondrial membrane potentials of **12b**. Bel-7402 cells were treated with **12b** for 48 h and then stained with JC-1. The changes of mitochondrial membrane potentials were analyzed by a flow cytometry.

2.2.7. Effects on apoptosis-related proteins

In general, apoptosis can be divided into two main pathways, intrinsic (the mitochondrial) pathway and extrinsic (the death receptor) pathway. Apoptosis through intrinsic pathway is usually mediated by a group of apoptosis related proteins. Bcl-2 family, an important protein family including Bcl-2, Bcl-xL and Bax, adjusts the mitochondrial membrane permeabization and eventually leads to apoptosis. Bcl-2 protein is an antiapoptotic protein and exerts inhibitory effects

on proapoptotic proteins through mediating permeability transition pore. Bcl-xL protein exhibits antiapoptotic effect by blocking the destruction of mitochondrial outer membrane caused by Bax. In addition, it also plays an important role in cell necrosis. While Bax protein (proapoptotic protein) can insert itself into mitochondrial outer membrane, uplift the permeabilization and induce the mitochondria to release cytochrome *c*. Caspase activation is also a key event in the initiation and execution of apoptosis in cells. With the releasing of cytochrome *c*, downstream apoptotic protein caspase-9 is activated. Upon activation, caspase-9 cleaves procaspase-3 and generates activated caspase-3 (cleaved caspase-3) directly, and then cleaves poly(ADP-ribose) polymerase (PARP), eventually causing the execution of apoptosis. In order to find out the mediative mechanism of aforementioned apoptosis related proteins behind **12b** induced apoptosis in Bel-7402 cells, corresponding Western blot analysis was conducted. As shown in Fig. 8, treatment with **12b** caused the increased expression of proapoptotic Bax, cleaved caspase-3, cytochrome *c* and cleaved PARP and suppressed procaspase-3, PARP, Bcl-2 and Bcl-xL. The results revealed that **12b** induced Bel-7402 cells apoptosis via mitochondria mechanism mediated by apoptotic related proteins.

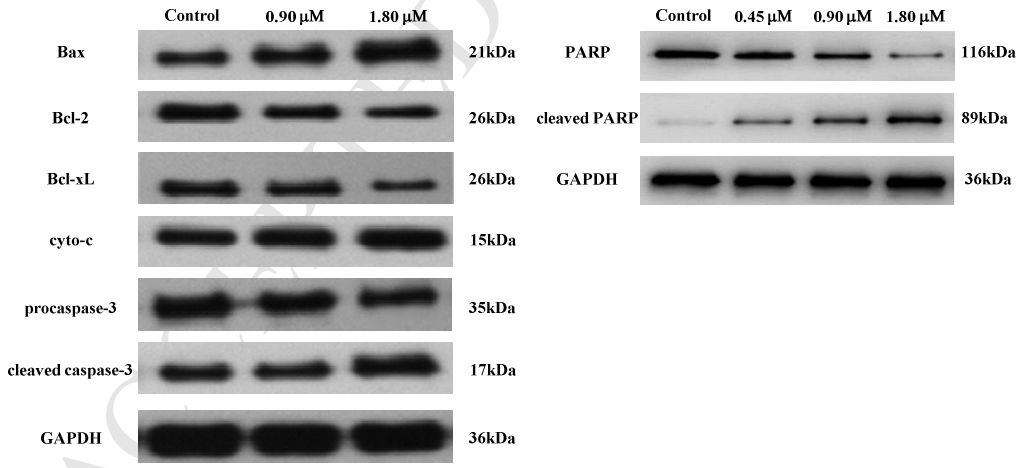

Fig. 8. Effects of **12b** on apoptosis-related proteins in Bel-7402 cells.

3. Conclusion

In this study, we designed and synthesized 14 H_2S-releasing derivatives. The antiproliferative activities of all derivatives were evaluated against four tumor and two normal cell lines. Most

derivatives displayed more potent antiproliferative activities than oridonin. Among them, compound **12b** showed the strongest antiproliferative effects, with IC_{50} values of 1.01, 0.88, 4.36 and 5.21 μM against K562, Bel-7402, SGC-7901 and A549 human cancer cell lines, respectively. Additionally, **12b** exhibited almost 24-fold less cytotoxicity against L-02 and PBMC cell lines, indicating good selectivity between cancer and normal cells. Hence, compound **12b** was selected for further mechanism study. The results demonstrated that the strong apoptotic effects of **12b** were attributed to G1 phase cell cycle arrest, collapse of mitochondrial membrane potential and mediation between proapoptotic and antiapoptotic proteins through mitochondrial pathway. In conclusion, **12b** merits further investigation as a potential candidate for anticancer therapeutics due to high efficiency and selectivity.

4. Experimental

4.1. Chemistry

Chemicals and solvents were commercially available. If required, further purification was abided by standard methods. Oridonin was purchased from Nanjing Zelang Biology Technology Co., Ltd with HPLC purity>98%. ^{1}H NMR and ^{13}C NMR spectra were measured on a Bruker 400 or 600 MHz spectrometer in the indicated solvents (TMS as internal standard): the values of the chemical shifts were expressed in δ (ppm) and the coupling constants (J) in Hz. Mass spectra were recorded on an Agilent 1100 LC-MSD-Trap-SL. High resolution mass spectra (HR-MS) were analyzed on Agilent Q-TOF B.05.01 (B5125.2).

4.1.1 General procedures to synthesize target derivatives

The preparation of ADT-OH was according to previous literature [82]. Oridonin (1 g, 2.76 mmol) was added in 20 mL of acetone and cooled to 0 °C. Jones reagent (3.2 mL, 8.28 mmol) was added dropwise and stirred at 0 °C for 0.5 h. The mixture was quenched by dropwise addition of isopropyl alcohol (1 mL) and extracted with DCM (3×30 mL). The combined organic layer was washed with brine, dried over anhydrous Na_2SO_4 and evaporated under reduced pressure to produce the crude compound **2**. Oridonin (182 mg, 0.50 mmol) was added into 10 mL acetone, then mixed with TsOH (43.1 mg, 0.25mmol), DMAP (30.5 mg, 0.25 mmol) and 2,2-dimethoxypropane (1.5 mL). The mixture was refluxed for 1.5 h and then concentrated in

vacuo to get compound **4**. **4** was dissolved in 5 mL DCM and mixed with 0.5 mL TEA, DMAP (catalytic amount) and 0.75 mL Ac_2O. After stirring at room temperature for 6h, extracted with DCM (3×30 mL), washed with brine, dried over anhydrous Na_2SO_4, and evaporated to give compound **5**. **5** was added to 10 mL of 10% HCl/THF (1:1) and the solution was stirred at room temperature for 4 h. Through post-processed as described above, compound **6** was got.

2 (108.6 mg, 0.3 mmol) was added in 5 mL anhydrous DCM, then reacted with α-thioctic acid (92.8 mg, 0.45 mmol) in the presence of EDCI (172.5 mg, 0.9mmol) and DMAP (7.4 mg, 0.06 mmol). The mixture was stirred at room temperature for 6 h and then extracted with DCM (3×30 mL), washed with brine, dried over anhydrous Na_2SO_4 and evaporated in vacuo. Compound **8** was obtained by purification with flash column chromatography (MeOH/DCM 1:200, v/v). Following the procedures described for **8**, compound **13** was prepared from **5**.

Different *ent*-kaurane diterpenoid derivatives (1.5 mmol) were dissolved in 5 mL anhydrous DCM and reacted with the corresponding anhydride (3.0 mmol), under the condition of TEA (1.04 mL, 7.5 mmol) and DMAP (91.6 mg, 0.75 mmol) for 5 h at room temperature. Then extracted with DCM (3×30 mL), washed with brine, dried over anhydrous Na_2SO_4 and evaporated in vacuo to get intermediates **10a-c** and **15a-c** without further purification. Intermediates **10a-c** and **15a-c** (0.6 mmol) were dissolved in 5 mL anhydrous DCM, reacted with ADT-OH (135.6 mg, 0.6 mmol) in the presence of EDCI (345.1 mg, 1.8 mmol) and DMAP (36.6 mg, 0.3 mmol). The mixture was stirred at room temperature for 6 h and then extracted with DCM (3×30 mL), washed with brine, dried over anhydrous Na_2SO_4, and evaporated in vacuo. Compounds **11a-c** and **16a-c** were acquired by purification with flash column chromatography (MeOH/DCM 1:300, v/v).

H_2S-releasing *ent*-kaurane diterpenoid derivatives **8**, **11a-c**, **13** and **16a-b** (0.2 mmol) were dissolved in 5 mL anhydrous THF, reacted with $Pb(OAc)_4$ (0.7 mmol) and Na_2CO_3 (1.6 mmol) at room temperature for 3 h. The mixture was extracted with DCM (3×30 mL), washed with brine, dried over anhydrous Na_2SO_4, and evaporated in vacuo to give corresponding crude products. Spirolactone-type 6,7-*seco*-*ent*-kaurane derivatives **9**, **12a-c**, **14** and **16a-b** were attained by purification with flash column chromatography (MeOH/DCM 1:400, v/v).

*4.1.1.1. Compound **9***. Pale yellow solid, yield: 42.1%. ^{1}H NMR ($CDCl_3$, 400 MHz), δ (ppm): 9.84

(1H, d, J = 3.4 Hz, -CHO), 6.23 (1H, s, 17-CH_2), 5.95 (1H, s, 14-CH), 5.58 (1H, s, 17-CH_2), 4.82, 4.44 (each 1H, d, J_A = J_B = 12.5 Hz, 20-CH_2), 3.14 (1H, s, 13-CH), 2.56 (2H, m, 8'-CH_2), 2.44 (2H, m, 2-CH_2), 2.26 (2H, m, 2'-CH_2), 1.82 (1H, m, -CH_2), 1.72-1.52 (7H, m, -CH_2), 1.48-1.36 (4H, m, -CH_2), 1.22 (3H, s, 18-CH_3),1.20 (3H, s, 19-CH_3); ^{13}C NMR ($CDCl_3$, 100 MHz), δ(ppm): 209.10, 201.91, 197.82, 172.87, 166.49, 146.64, 120.85, 73.71, 67.80, 61.50, 59.57, 52.43, 44.79, 41.63, 37.16, 36.02, 34.11, 33.54, 30.48, 29.68, 29.47, 29.30, 28.60, 27.73, 26.37, 25.81, 23.99, 18.83; $C_{28}H_{38}O_7S_2$ MS (ESI) *m/z* calcd for $[M+K]^+$ 587.2, found 587.3.

*4.1.1.2. Compound **11a***. Orange red solid, yield: 26.2%. ^{1}H NMR ($CDCl_3$, 400 MHz), δ (ppm): 7.67, 7.24 (each 2H, d, J_A = J_B = 8.7 Hz, Ar-H), 7.41 (1H, s, 8''-CH), 6.24 (1H, s, 17-CH_2), 6.00 (1H, s, 17-CH_2), 5.61 (1H, s, 7-OH), 5.42 (1H, d, J = 11.8 Hz, 6-OH), 4.31, 4.02 (each 1H, d, J = 10.7 Hz, 20-CH_2), 3.76 (1H, dd, J = 11.7, 8.9 Hz, 6-CH), 3.10 (1H, d, J = 9.2 Hz, 13-CH), 2.88 (2H, m, 2'-CH_2), 2.69 (2H, m, 3'-CH_2), 2.59-2.42 (2H, m, -CH_2), 2.38-2.29 (1H, m, -CH_2), 2.21 (1H, dd, J = 13.7, 4.7 Hz, -CH), 1.94 (2H, m, -CH_2), 1.77-1.58 (2H, m, -CH_2), 1.31 (1H, m, -CH_2), 1.19 (3H, s, 18-CH_3), 0.99 (3H, s, 19-CH_3); ^{13}C NMR ($CDCl_3$, 100 MHz), δ (ppm): 215.46, 211.51, 204.87, 170.71, 170.37, 153.49, 149.44, 136.01, 129.21, 128.18 (×2), 122.88 (×2), 122.20, 96.85, 74.25, 73.46, 64.93, 61.38, 59.61, 50.69, 48.51, 41.50, 38.31, 35.71, 33.37, 32.84, 30.50, 30.06, 29.37, 29.07, 23.16, 19.19; HRMS (ESI) *m/z* calcd for $C_{33}H_{34}O_9S_3$ $[M+Na]^+$ 693.1257, found 693.1289.

*4.1.1.3. Compound **11b***. Orange red solid, yield: 29.5%. ^{1}H NMR ($CDCl_3$, 400 MHz), δ (ppm): 7.68, 7.22 (each 2H, d, J_A = J_B = 8.68 Hz, Ar-H), 7.41 (1H, s, 8''-H), 6.26 (1H, s, 17-CH_2), 5.97 (1H, s, 17-CH_2), 5.64 (1H, s, 7-OH), 5.41 (1H, d, J = 11.76 Hz, 6-OH), 4.31, 4.03 (each 1H, d, J = 10.64 Hz, 20-CH_2), 3.77 (1H, dd, J = 11.5, 8.8 Hz, 6-CH), 3.10 (1H, d, J = 9.3 Hz, 13-CH), 2.65 (2H, td, J = 3.56, 7.4 Hz, 3'-CH_2), 2.43 (2H, t, J = 7.16 Hz, 4'-CH_2), 2.22 (1H, dd, J = 13.5, 4.4 Hz, -CH), 2.03 (2H, t, J = 6.84 Hz, 2'-CH_2), 1.94 (2H, m, -CH_2), 1.78-1.60 (2H, m, -CH_2), 1.32 (1H, m, -CH_2), 1.19 (3H, s, 18-CH_3), 1.00 (3H, s, 19-CH_3); ^{13}C NMR ($CDCl_3$, 100 MHz), δ (ppm): 215.47, 211.54, 204.85, 171.33, 170.89, 153.49, 149.48, 136.01, 129.17, 128.20 (×2), 122.92 (×2), 122.14, 96.90, 74.15, 73.38, 64.95, 61.35, 59.68, 53.47, 50.68, 48.53, 41.55, 38.34, 35.73, 33.28, 33.14,

32.85, 30.50, 30.05, 23.18, 19.55, 19.18; HRMS (ESI) *m/z* calcd for $C_{34}H_{36}O_9S_3$ $[M+Na]^+$ 707.1414, found 707.1451.

4.1.1.4. Compound ***11c***. Orange red solid, yield: 31.6%. ^{1}H NMR ($CDCl_3$, 400 MHz), δ (ppm): 7.98 (1H, dd, J = 7.4, 1.7 Hz, 6'-H), 7.79 (1H, dd, J = 7.4, 1.7 Hz, 3'-H), 7.75 (2H, d, J = 8.7 Hz, Ar-H), 7.58 (2H, m, 4', 5'-H), 7.45 (2H, d, J = 8.7 Hz, Ar-H), 7.44 (1H, s, 8"-H), 6.08 (1H, s, 17-CH_2), 6.08 (1H, s, 14-CH), 5.42 (1H, s, 17-CH_2), 4.70 (1H, d, J = 10.8 Hz, 6-OH), 4.63 (1H, s, 14-CH), 3.85, 3.27 (each 1H, d, J = 9.6 Hz, 20-CH_2), 2.62 (1H, m, -CH_2), 2.50 (1H, m, -CH_2), 2.28 (1H, m, -CH_2), 1.95-1.59 (5H, m, -CH_2), 1.51 (3H, s, 18-CH_3), 1.28 (3H, s, 19-CH_3); ^{13}C NMR ($CDCl_3$, 100 MHz), δ (ppm): 215.51, 208.20, 202.90, 200.66, 171.77, 165.44, 153.90, 148.55, 136.06, 131.76, 131.72, 131.68, 131.01, 130.45, 129.74, 129.40, 128.62, 128.28 (×2), 123.05 (×2), 120.08, 93.20, 74.23, 67.62, 60.97, 58.46, 49.52, 41.04, 40.86, 36.22, 33.85, 33.40, 29.64, 22.70, 18.19; HRMS (ESI) *m/z* calcd for $C_{37}H_{34}O_9S_3$ $[M+H]^+$ 717.1286, found 717.1288.

4.1.1.5. Compound ***12a***. Orange red solid, yield: 21.8%. ^{1}H NMR ($CDCl_3$, 600 MHz), δ (ppm): 9.85 (1H, d, J = 3.4 Hz, -CHO), 7.66, 7.23 (each 2H, d, J_A = J_B = 8.6 Hz, Ar-H), 7.40 (1H, s, 8"-CH), 6.24 (1H, s, 17-CH_2), 6.04 (1H, s, 14-CH), 5.59 (1H, s, 17-CH_2), 4.82, 4.48 (each 1H, d, J_A = J_B = 12.4 Hz, 20-CH_2), 3.16 (1H, d, J = 7.6 Hz, 13-CH), 2.94 (1H, m, 2'-CH_2), 2.81 (1H, m, 2'-CH_2), 2.72 (2H, m, 3'-CH_2), 2.60 (2H, m, 2-CH_2), 2.48-2.35 (4H, m, -CH_2), 1.86 (2H, m, -CH_2), 1.73-1.62 (4H, m, -CH_2), 1.42 (2H, m, -CH_2), 1.25 (3H, s, 18-CH_3), 1.22 (3H, s, 19-CH_3); ^{13}C NMR ($CDCl_3$, 150 MHz), δ (ppm): 215.53, 208.90, 201.89, 197.81, 171.81, 171.63, 170.41, 166.62, 153.55, 146.63, 136.03, 129.19, 128.86, 128.18 (×2), 122.95 (×2), 121.31, 74.13, 67.86, 61.26, 59.59, 52.52, 44.88, 41.53, 37.05, 36.25, 34.18, 30.63, 29.71, 29.53, 29.04, 28.99, 25.78, 18.81; HRMS (ESI) *m/z* calcd for $C_{33}H_{32}O_9S_3$ $[M+H]^+$ 669.1286, found 669.1299.

4.1.1.6. Compound ***12b***. Orange red solid, yield: 24.6%. ^{1}H NMR ($CDCl_3$, 600 MHz), δ (ppm): 9.86 (1H, d, J = 3.4 Hz, -CHO), 7.67, 7.23 (each 2H, d, J_A = J_B = 8.6 Hz, Ar-H), 7.41 (1H, s, 8"-CH), 6.25 (1H, s, 17-CH_2), 6.03 (1H, s, 14-CH), 5.59 (1H, s, 17-CH_2), 4.86, 4.48 (each 1H, d, J_A = J_B = 12.4 Hz, 20-CH_2), 3.16 (1H, d, J = 7.3 Hz, 13-CH), 2.65 (2H, m, 3'-CH_2), 2.60 (1H, m, 2'-CH_2), 2.45 (2H, m, 4'-CH_2), 2.38 (1H, m, 2'-CH_2), 2.01 (2H, m, -CH_2), 1.85 (1H, m, -CH_2),

1.69 (4H, m, -CH_2), 1.43 (1H, m, -CH_2), 1.25 (3H, s, 18-CH_3), 1.22 (3H, s, 19-CH_3); ^{13}C NMR ($CDCl_3$, 150 MHz), δ (ppm): 215.51, 209.17, 201.95, 197.81, 172.48, 171.91, 171.07, 166.64, 153.62, 146.60, 136.00, 129.09, 128.86, 128.20 (×2), 123.03 (×2), 121.07, 73.93, 67.85, 61.46, 59.65, 52.46, 44.85, 41.61, 37.15, 36.13, 34.14, 32.98, 32.73, 30.55, 29.49, 19.40, 18.83; HRMS (ESI) *m*/*z* calcd for $C_{34}H_{34}O_9S_3$ $[M+H]^+$ 683.1443, found 683.1436.

*4.1.1.7. Compound **12c***. Orange red solid, yield: 14.8%. ^{1}H NMR ($CDCl_3$, 600 MHz), δ (ppm): 9.86 (1H, d, J = 3.4 Hz, -CHO), 7.67, 7.23 (each 2H, d, J_A = J_B = 8.6 Hz, Ar-H), 7.41 (1H, s, 8"-CH), 6.25 (1H, s, 17-CH_2), 6.03 (1H, s, 14-CH), 5.59 (1H, s, 17-CH_2), 4.86, 4.48 (each 1H, d, J_A = J_B = 12.4 Hz, 20-CH_2), 3.16 (1H, d, J = 7.3 Hz, 13-CH), 2.65 (2H, m, 3'-CH_2), 2.60 (1H, m, 2'-CH_2), 2.45 (2H, m, 4'-CH_2), 2.38 (1H, m, 2'-CH_2), 1.86 (2H, m, -CH_2), 1.80-1.60 (5H, m, -CH_2), 1.44 (1H, m, -CH_2), 1.25 (3H, s, 18-CH_3), 1.22 (3H, s, 19-CH_3); ^{13}C NMR ($CDCl_3$, 150 MHz), δ (ppm): 215.54, 208.89, 201.81, 197.76, 171.74, 166.42, 166.16, 153.81, 146.70, 136.09, 132.37, 131.80, 131.49, 130.28, 129.97, 129.74, 129.43, 129.16, 128.28 (×2), 123.02 (×2), 121.37, 74.87, 67.86, 61.24, 59.64, 52.69, 45.16, 41.50, 37.02, 36.36, 34.18, 30.69, 29.61, 25.73, 18.80; HRMS (ESI) *m*/*z* calcd for $C_{37}H_{32}O_9S_3$ $[M+Na]^+$ 739.1106, found 739.1110.

*4.1.1.8. Compound **13***. Pale yellow solid, yield: 19.8%. ^{1}H NMR ($CDCl_3$, 400 MHz), δ (ppm): 6.15 (1H, s, 17-CH_2), 5.80 (1H, s, 14-CH), 5.51 (1H, s, 17-CH_2), 4.63 (1H, q, J = 10.6 Hz, 1-CH), 4.26, 4.18 (each 1H, d, J = 10.6 Hz, 20-CH_2), 3.78 (1H, brs, -OH), 3.17 (1H, d, J = 9.7 Hz, 13-CH), 2.53 (1H, dq, J = 6.4, 12.6 Hz, 8'-CH), 2.44 (1H, dt, J = 6.4, 12.6 Hz, 8'-CH), 2.30 (3H, t, J = 7.5 Hz, 2', 7'-CH, -CH_2), 1.99 (3H, s, -CH_3), 1.93-1.23 (20H, m, -CH_2), 1.12 (6H, s, 18, 19-CH_3); ^{13}C NMR ($CDCl_3$, 100 MHz), δ (ppm): 206.21, 171.81, 169.87, 149.37, 120.47, 96.10, 76.40, 75.37, 73.77, 63.53, 61.48, 60.24, 56.21, 53.68, 41.33, 41.04, 40.21, 39.75, 38.47, 38.13, 34.45, 34.35, 33.58, 32.36, 30.20, 28.54, 25.17, 24.39, 21.54, 17.96; HRMS (ESI) *m*/*z* calcd for $C_{30}H_{42}O_8S_2$ $[M+Na]^+$ 617.2219, found 617.2204.

*4.1.1.9. Compound **14***. Pale yellow solid, yield: 39.1%. ^{1}H NMR ($CDCl_3$, 400 MHz), δ (ppm): 9.79 (1H, d, J = 4.7 Hz, -CHO), 6.23 (1H, s, 17-CH_2), 5.79 (1H, s, 14-CH), 5.59 (1H, s, 17-CH_2), 5.10, 4.76 (each 1H, d, J_A = J_B = 12.5 Hz, 20-CH_2), 4.63 (1H, m, 1-CH), 2.98 (1H, d, J = 7.4 Hz,

13-CH), 2.31-2.24 (2H, m, -CH_2), 2.23 (2H, t, J = 4.4 Hz, 2'-CH_2), 2.10 (3H, s, -CH_3), 2.06 (2H, m, -CH_2), 1.96-1.76 (4H, m, -CH_2), 1.71-1.31 (10H, m, -CH_2), 1.21 (3H, s, 18-CH_3), 0.99 (3H, s, 19-CH_3); ^{13}C NMR ($CDCl_3$, 100 MHz), δ (ppm): 202.41, 196.99, 172.60, 170.37, 166.59, 146.77, 121.45, 74.44, 72.23, 66.34, 62.68, 62.60, 61.62, 59.89, 55.42, 53.44, 45.63, 43.57, 42.16, 39.31, 35.46, 34.01, 32.86, 29.96, 28.69, 27.75, 23.93, 23.87, 21.44, 17.45; $C_{30}H_{40}O_8S_2$ MS (ESI) *m/z* calcd for $[M+K]^+$ 631.2, found 631.3.

*4.1.1.10. Compound **16a***. Orange red solid, yield: 18.8%. ^{1}H NMR ($CDCl_3$, 400 MHz), δ (ppm): 7.68, 7.24 (each 2H, d, $J_A = J_B$ = 8.6 Hz, Ar-H), 7.40 (1H, s, 8"-CH), 6.14 (1H, s, 17-CH_2), 6.08 (1H, d, J = 10.8 Hz, 6-OH), 5.93 (1H, s, 14-CH), 5.50 (1H, s, 17-CH_2), 4.63 (1H, dd, J = 11.1, 5.5 Hz, 1-CH), 4.30, 4.20 (each 1H, d, $J_A = J_B$ = 10.6 Hz, 20-CH_2), 3.91 (1H, brs, -OH), 3.77 (1H, dd, J = 10.3, 6.9 Hz, 6-CH), 3.14 (1H, d, J = 10.0 Hz, 13-CH), 2.90 (2H, m, 3'-CH_2), 2.72 (2H, m, 2'-CH_2), 2.52 (1H, m, -CH_2), 1.78 (1H, m, -CH_2), 1.48 (2H, m, -CH_2), 1.37-1.29 (4H, m, -CH_2), 1.99 (3H, s, -CH_3), 1.13 (6H, s, 18,19-CH_3); ^{13}C NMR ($CDCl_3$, 100 MHz), δ (ppm): 215.53, 206.10, 171.57, 170.72, 170.19, 169.84, 153.45, 149.42, 136.06, 129.30, 128.17(×2), 122.84(×2), 120.74, 95.91, 75.78, 75.36, 74.37, 63.59, 61.71, 59.89, 53.87, 41.18, 39.79, 38.16, 33.57, 32.46, 30.27, 29.70, 29.41, 29.07, 25.15, 21.65, 21.52, 18.13; HRMS (ESI) *m/z* calcd for $C_{35}H_{38}O_{10}S_3$ $[M+Na]^+$ 737.1525, found 737.1534.

*4.1.1.11. Compound **16b***. Orange red solid, yield: 23.4%. ^{1}H NMR ($CDCl_3$, 400 MHz), δ (ppm): 7.68, 7.22 (each 2H, d, $J_A = J_B$ = 8.7 Hz, Ar-H), 7.40 (1H, s, 8"-CH), 6.17 (1H, s, 17-CH_2), 6.08 (1H, d, J = 10.6 Hz, 6-OH), 5.89 (1H, s, 14-CH), 5.52 (1H, s, 17-CH_2), 4.63 (1H, dd, J = 11.2, 5.6 Hz, 1-CH), 4.30, 4.20 (each 1H, d, $J_A = J_B$ = 10.6 Hz, 20-CH_2), 4.09 (1H, brs, -OH), 3.78 (1H, t, J = 7.7 Hz, 6-CH), 3.16 (1H, d, J = 9.9 Hz, 13-CH), 2.65 (2H, td, J = 7.3, 2.5 Hz, 3'-CH_2), 2.44 (2H, t, 2'-CH_2), 2.01 (3H, s, -CH_3), 1.78 (1H, m, -CH_2), 1.48 (2H, m, -CH_2), 1.38-1.28 (4H, m, -CH_2), 1.13 (6H, s, 18,19-CH_3); ^{13}C NMR ($CDCl_3$, 100 MHz), δ (ppm): 215.52, 206.11, 171.64, 171.32, 170.72, 169.86, 153.44, 149.43, 136.04, 129.23, 128.20(×2), 122.89(×2), 120.64, 95.98, 75.85, 75.36, 74.13, 63.58, 61.62, 59.97, 53.78, 41.18, 39.76, 38.13, 32.43, 30.25, 25.16, 21.61, 21.55, 19.59, 18.08; HRMS (ESI) *m/z* calcd for $C_{36}H_{40}O_{10}S_3$ $[M+Na]^+$ 751.1682, found 751.1649.

*4.1.1.12. Compound **16c***. Orange red solid, yield: 13.1%. ^{1}H NMR ($CDCl_3$, 400 MHz), δ (ppm): 7.95 (1H, m, 6'-H), 7.75, 7.43 (each 2H, d, $J_A = J_B$ = 8.6 Hz, Ar-H), 7.72 (1H, m, 3'-H), 7.62 (2H, m, 4'-H,5'-H), 7.40 (1H, s, 8''-H), 6.07 (1H, s, 7-OH), 6.07, 5.39 (2H, s, 17-CH_2), 4.65 (1H, m, 1-CH), 4.32, 4.21 (each 1H, d, J = 10.6 Hz, 20-H), 4.00 (1H, brs, -OH), 3.78 (1H, m, 6-CH), 3.37 (1H, d, J = 9.7 Hz, 13-CH), 2.01 (3H, s, -CH_3), 1.78 (1H, m, -CH_2), 1.49 (2H, m, -CH_2), 1.39-1.30 (4H, m, -CH_2), 1.13 (6H, s, 18,19-CH_3); ^{13}C NMR ($CDCl_3$, 100 MHz), δ (ppm): 215.52, 206.12, 171.51, 169.85, 166.02, 164.77, 153.65, 149.41, 136.13, 132.60, 132.45, 131.53, 129.82, 129.60, 129.54, 129.04, 128.22 (×2), 123.03 (×2), 120.76, 96.02, 75.36, 74.22, 63.62, 61.74, 60.04, 53.94, 40.69, 39.82, 38.16, 33.58, 32.44, 30.26, 29.70, 25.17, 21.63, 21.57, 18.10; HRMS (ESI) *m/z* calcd for $C_{39}H_{38}O_{10}S_3$ $[M+Na]^+$ 785.1525, found 785.1526.

*4.1.1.13. Compound **17a***. Orange red solid, yield: 7.5%. ^{1}H NMR ($CDCl_3$, 400 MHz), δ (ppm): 9.85 (1H, d, J = 3.4 Hz, -CHO), 9.79 (1H, d, J = 4.6 Hz, -CHO), 7.66, 7.23 (each 2H, d, $J_A = J_B$ = 8.7 Hz, Ar-H), 7.39 (1H, s, 8''-CH), 6.23 (1H, s, 17-CH_2), 5.81 (1H, s, 14-CH), 5.59 (1H, s, 17-CH_2), 5.11, 4.76 (each 1H, d, $J_A = J_B$ = 12.4 Hz, 20-CH_2), 4.63 (1H, m, 1-CH), 3.02 (1H, d, J = 7.7 Hz, 13-CH), 2.93 (1H, m, 2'-CH_2), 2.82 (1H, m, 2'-CH_2), 2.73 (2H, m, 3'-CH_2), 2.33-2.23 (2H, m, -CH_2), 2.10 (3H, s, -CH_3), 1.90 (2H, m, -CH_2), 1.71-1.49 (6H, m, -CH_2), 1.21 (3H, s, 18-CH_3), 1.01 (3H, s, 19-CH_3); ^{13}C NMR ($CDCl_3$, 100 MHz), δ (ppm): 215.50, 202.31, 196.82, 171.71, 171.22, 170.40, 166.68, 153.57, 146.77, 136.01, 129.18, 128.15 (×2), 122.87 (×2), 121.87, 74.55, 72.59, 66.44, 62.35, 59.80, 45.69, 43.58, 41.99, 39.44, 34.04, 32.90, 29.94, 29.21 (×2), 24.09 (×2), 21.41, 17.53; HRMS (ESI) *m/z* calcd for $C_{35}H_{36}O_{10}S_3$ $[M+H]^+$ 713.1549, found 713.1546.

*4.1.1.14. Compound **17b***. Orange red solid, yield: 10.1%. ^{1}H NMR ($CDCl_3$, 400 MHz), δ (ppm): 9.80 (1H, d, J = 4.7 Hz, -CHO), 7.67, 7.22 (each 2H, d, $J_A = J_B$ = 8.6 Hz, Ar-H), 7.41 (1H, s, 8''-CH), 6.26 (1H, s, 17-CH_2), 5.83 (1H, s, 14-CH), 5.60 (1H, s, 17-CH_2), 5.12, 4.77 (each 1H, d, $J_A = J_B$ = 12.4 Hz, 20-CH_2), 4.64 (1H, m, 1-CH), 3.01 (1H, d, J = 7.7 Hz, 13-CH), 2.65 (2H, m, 4'-CH_2), 2.45 (2H, m, 2'-CH_2), 2.28-2.22 (2H, m, -CH_2), 2.13 (1H, s, -CH_3), 2.10 (1H, d, J = 4.8 Hz, -CH), 2.03 (2H, m, 3'-CH_2), 1.22 (3H, s, 18-CH_3), 1.01 (3H, s, 19-CH_3); ^{13}C NMR ($CDCl_3$, 100 MHz), δ (ppm): 215.54, 202.34, 172.13, 171.04, 170.46, 166.73, 153.62, 146.80, 136.01,

128.17 (×2), 123.00 (×2), 121.70, 74.53, 72.26, 66.40, 62.49, 59.89, 45.69, 43.59, 42.09, 39.43, 34.04, 32.97 (×2), 29.96, 29.71, 23.93 (×2), 21.44, 19.45, 17.52; HRMS (ESI) *m*/*z* calcd for $C_{36}H_{38}O_{10}S_3$ $[M+H]^+$ 727.1705, found 727.1703.

4.2. MTT assay

The antiproliferative activities were examined by the MTT assay following the method described previously. All selected cell lines were incubated with target compounds for different concentrations (64, 16, 4, 1, 0.25, 0.0625 and 0.015625 μM) through a standard 96-well plates. After 72 h, MTT solution (20 mL, 5 mg/mL) and DMSO (150 mL/well) were added, then incubated for 10 min at room temperature. After that, the absorbance (OD) data of each well at 490 nm wavelength were measured by a Microplate Reader (BIO-RAD). Four human cancer and two normal cell lines were selected for the assay, and half inhibition rates (IC_{50}) were calculated.

4.3. H_2S release experiment

Sodium phosphate buffer was used to prepare the stock solution of Na_2S (20 mM) in 100 mL volumetric flask. Aliquots of Na_2S stock solution were transferred into a 50 mL volumetric flask to obtain standard solutions of 5, 10, 20, 40, 60, 80, 100 and 150 μM, respectively. 1 mL of each standard solutions were added to react with the methylene blue (MB^+) cocktail (200 μL of 30 mM $FeCl_3$ in 1.2M HCl, 200 μL of 20 mM *N*,*N*-dimethyl-1,4-phenylenediamine sulfate in 7.2M HCl and 100 μL of 1%w/v of $Zn(OAc)_2$ in H_2O) at room temperature for 20 min in a triplicate manner [83]. The mixture was measured at 670 nm in UV-Vis spectrophotometer and then the Na_2S calibration curve was obtained. In order to promote compounds to release H_2S, TCEP or L-cysteine was used as an accelerator. All compounds were dissolved in THF solution (40 mM) and added into phosphate buffer in the presence of TCEP or L-cysteine (1 mM). Then 2 mL mixture was transferred to colorimetric cuvette containing methylene blue (MB^+) cocktail in designated time. After 20 min incubation, the absorbance of each compound was analyzed by UV-Vis spectrophotometer at 670 nm. The H_2S concentration of each derivative was calculated through standard curve.

4.4. Cell cycle analysis

Effects of **12b** on cell cycle arrest in Bel-7402 cells were tested and DNA content of cell

nuclei was measured via flow cytometry [84]. Bel-7402 cells were incubated in 6-well plates at 37 °C for 24 h. Then **12b** was dissolved in DMSO and joined cell culture with designated concentrations in triplicate manner. While DMSO was used as control. After 48 h incubation, all cells were centrifuged and fixed with 70% ethanol at 4 °C overnight and suspended again in PBS mixed with 100 mL RNase A and 400 mL PI. Cell cycle distribution of DNA content was evaluated via flow cytometer (FACS Calibur Becton-Dickinson, Franklin Lake, NJ, USA).

4.5. Hoechst 333258 staining

Hoechst 33258 staining assay was used to observe the morphology change of nuclei. Bel-7402 cells were cultured in 6-well plates at 37 °C with 2 mL medium. After 24 h of incubation, **12b** of designated concentrations (0, 0.45, 0.90 and 1.80 μM) was added for another 48 h incubation. Cells were harvested by mild trypsinization, collected by centrifugation and washed twice with PBS. After that, 500 μL of Hoechst mixture (2 mg/mL) in PBS was added for 15 min at room temperature in darkness in order to stain aforementioned cells. Finally, cells were washed by PBS and assessed via a fluorescence microscope.

4.6. Cell apoptosis assay

Bel-7402 cells were treated with designated concentrations of **12b** (0, 0.45, 0.90 and 1.80 μM) for 24 h incubation in 6-well plates. Then, cells were washed twice with PBS and suspended in annexin V binding buffer. The mixture was incubated with V-FITC and PI at room temperature for 15 min in dark. After that, cells with double-staining were analyzed by flow cytometry to detect apoptotic cells.

4.7. Mitochondrial membrane potential assay

Bel-7402 cells were cultured in 6-well plates with different concentrations of **12b** (0, 0.45, 0.90 and 1.80 μM) for 48 h, then washed with PBS and stained with JC-1 at room temperature in darkness. A flow cytometry was used to measure the number of cells with collapsed mitochondrial membrane potentials.

4.8. Western blot assay

Bel-7402 cells were treated with **12b** (0, 0.45, 0.90 and 1.80 μM) in triplicate for 48 h. Following the measurement of protein level, sodium dodecyl sulfate polyacrylamide gel

electrophoresis (10% gel, SDS-PAGE) was applied to split each cell lysates, and then transferred onto nitrocellulose membranes. Afterwards membranes were blocked with 5% of nonfat milk, incubated with monoclonal antibodies for 12 h at 4 °C. Then washed with TBST, incubated with appropriate second antibodies and followed by chemiluminescence detection [85]. Protein visualization was analyzed by Keygen ECL system (KeyGEN Biotech, Nanjing, China) while resulting images were obtained by Clinx ChemiScope chemiluminescence imaging system. ChemiScope analysis program was used to gain relative optical densities for individual protein.

Acknowledgment

This paper was financially supported by the National Natural Science Foundation of China (21772124, 21502121), Natural Science Foundation of Liaoning Province (20170540858), General Scientific Research Projects of Department of Education in Liaoning Province (2017LQN05), Key Laboratory of Quality Control of TCM of Liaoning Province (17-137-1-00) and Career Development Support Plan for Young and Middle-aged Teachers in Shenyang Pharmaceutical University.

References

[1] T. Rodrigues, D. Reker, P. Schneider, G. Schneider, Counting on natural products for drug design, Nat. Chem. 8 (2016) 531-541.

[2] D.J. Newman, G.M. Cragg, Natural products as sources of new drugs from 1981 to 2014, J. Nat. Prod. 79 (2016) 629-661.

[3] J. Yang, W.G. Wang, H.Y. Wu, X. Du, X.N. Li, Y. Li, J.X. Pu, H.D. Sun, Bioactive enmein-type *ent*-kaurane diterpenoids from *Isodon phyllostachys*, J. Nat. Prod. 79 (2016) 132-140.

[4] X. Luo, J.X. Pu, W.L. Xiao, Y. Zhao, X.M. Gao, X.N. Li, H.B. Zhang, Y.Y. Wang, Y. Li, H.D. Sun, Cytotoxic *ent*-kaurane diterpenoids from *Isodon rubescens* var. *lushiensis*, J. Nat. Prod. 73 (2010) 1112-1116.

[5] S.S. Hong, S.A. Lee, X.H. Han, J.S. Hwang, C. Lee, D. Lee, J.T. Hong, Y. Kim, H. Lee, B.Y. Hwang, *ent*-Kaurane diterpenoids from *Isodon japonicus*, J. Nat. Prod. 71 (2008) 1055-1058.

[6] J. Zou, X. Du, G. Peng, Y.M. Shi, W.G. Wang, R. Zhan, L.M. Kong, X.N. Li, Y. Li, J.X. Pu, H.D. Sun, Ternifolide A, a new diterpenoid rossessing a rare macrolide motif from *Isodon ternifolius*, Org. Lett. 14 (2012) 3210-3213.

[7] Q.B. Han, S. Cheung, J. Tai, C.F. Qiao, J.Z. Song, T.F. Tso, H.D. Sun, H.X. Xu, Maoecrystal Z, a cytotoxic diterpene from *Isodon eriocalyx* with a unique skeleton, Org. Lett. 8 (2006) 4727-4730.

[8] W. Zhao, J.X. Pu, X. Du, J. Su, X.N. Li, J.H. Yang, Y.B. Xue, Y. Li, W.L. Xiao, H.D. Sun, Structure and cytotoxicity of diterpenoids from *Isodon adenolomus*, J. Nat. Prod. 74 (2011) 1213-1220.

[9] J. Zou, L.T. Pan, Q.J. Li, J.H. Zhao, J.X. Pu, P. Yao, N.B. Gong, Y. Lu, T.P. Kondratyuk, J.M. Pezzuto, H.H.S. Fong, H.J. Zhang, H.D. Sun, Rubesanolides A and B: diterpenoids from *Isodon rubescens*, Org. Lett. 13 (2011) 1406-1409.

[10] W.G. Wang, X. Du, X.N. Li, H.Y. Wu, X. Liu, S.Z. Shang, R. Zhan, C.Q. Liang, L.M. Kong, Y. Li, J.X. Pu, H.D. Sun, New Bicyclo[3.1.0]hexane unit *ent*-kaurane diterpene and its *seco*-derivative from *Isodon eriocalyx* var. *laxiflora*, Org. Lett. 14 (2012) 1302-1305.

[11] J. Xu, J. Yang, Q. Ran, L. Wang, J. Liu, Z. Wang, X. Wu, W. Hua, S. Yuan, L. Zhang, M. Shen, Y. Ding, Synthesis and biological evaluation of novel 1-*O*- and 14-*O*-derivatives of oridonin as potential anticancer drug candidates, Bioorg. Med. Chem. Lett. 18 (2008) 4741-4744.

[12] D. Li, L. Wang, H. Cai, Y. Zhang, J. Xu, Synthesis and biological evaluation of novel furozan-based nitric oxide-releasing derivatives of oridonin as potential anti-tumor agents, Molecules 17 (2012) 7556-7568.

[13] C.Y. Ding, Y.S. Zhang, H.J. Chen, C. Wild, T.Z. Wang, M.A. White, Q. Shen, J. Zhou, Overcoming synthetic challenges of oridonin A-ring structural diversification: regio- and stereoselective installation of azides and 1,2,3-triazoles at the C-1, C-2, or C-3 position, Org. Lett. 15 (2013) 3718-3721.

[14] C. Ding, Y. Zhang, H. Chen, Z. Yang, C. Wild, N. Ye, C.D. Ester, A. Xiong, M.A. White, Q. Shen, J. Zhou, Oridonin ring A-based diverse constructions of enone functionality: identification of novel dienone analogues effective for highly aggressive breast cancer by inducing apoptosis, J. Med. Chem. 56 (2013) 8814-8825.

[15] C. Ding, Y. Zhang, H. Chen, Z. Yang, C. Wild, L. Chu, H. Liu, Q. Shen, J. Zhou, Novel nitrogen-enriched oridonin analogues with thiazole-fused A-ring: protecting group-free synthesis, enhanced anticancer profile, and improved aqueous solubility, J. Med. Chem. 56 (2013) 5048-5058.

[16] S. Xu, L. Pei, C. Wang, Y.K. Zhang, D. Li, H. Yao, X. Wu, Z.S. Chen, Y. Sun, J. Xu, Novel hybrids of natural oridonin-bearing nitrogen mustards as potential anticancer drug candidates, ACS Med. Chem. Lett. 5 (2014) 797-802.

[17] S. Xu, D. Li, L. Pei, H. Yao, C. Wang, H. Cai, H. Yao, X. Wu, J. Xu, Design, synthesis and antimycobacterial activity evaluation of natural oridonin derivatives, Bioorg. Med. Chem. Lett. 24 (2014) 2811-2814.

[18] S. Xu, H. Yao, S. Luo, Y.K. Zhang, D.H. Yang, D. Li, G. Wang, M. Hu, Y. Qiu, X. Wu, H. Yao, W. Xie, Z.S. Chen, J. Xu, A novel potent anticancer compound optimized from a natural oridonin scaffold induces apoptosis and cell cycle arrest through the mitochondrial pathway, J. Med. Chem. 60 (2017) 1449-1468.

[19] Y. Ding, C. Ding, N. Ye, Z. Liu, E.A. Wold, H. Chen, C. Wild, Q. Shen, J. Zhou, Discovery and development of natural product oridonin-inspired anticancer agents, Eur. J. Med. Chem. 122 (2016) 102-117.

[20] D. Li, T. Han, S. Xu, T. Zhou, K. Tian, X. Hu, K. Cheng, Z. Li, H. Hua, J. Xu, Antitumor and antibacterial derivatives of oridonin: a main composition of Dong-Ling-Cao, Molecules 21 (2016) 575.

[21] E. Fujita, T. Fujita, H. Katayama, M. Shibuya, T. Shingu, Terpenoids. Part XV. Structure and absolute configuration oridonin isolated from *Isodon japonicus* and *Isodon trichocarpus*, J. Chem. Soc. C 21 (1970) 1674–1681.

[22] G.B. Zhou, H. Kang, L. Wang, L. Gao, P. Liu, J. Xie, F.X. Zhang, X.Q. Weng, Z.X. Shen, J. Chen, L.J. Gu, M. Yan, D.E. Zhang, S.J. Chen, Z.Y. Wang, Oridonin, a diterpenoid extracted from medicinal herbs, targets AML1-ETO fusion protein and shows potent antitumor activity with low adverse effects on t(8;21) leukemia in vitro and in vivo, Blood 109 (2007) 3441-3450.

[23] X. Qi, D. Zhang, X. Xu, F. Feng, G. Ren, Q. Chu, Q. Zhang, K. Tian, Oridonin nanosuspension was more effective than free oridonin on G_2/M cell cycle arrest and apoptosis in the human pancreatic cancer PANC-1 cell line, Int. J. Nanomed. 7 (2012) 1793-1804.

[24] Y. Lu, Y. Sun, J. Zhu, L. Yu, X. Jiang, J. Zhang, X. Dong, B. Ma, Q. Zhang, Oridonin exerts anticancer effect on osteosarcoma by activating PPAR-γ and inhibiting Nrf2 pathway, Cell Death Dis. 9 (2018) 15.

[25] Z. Yao, F. Xie, M. Li, Z. Liang, W. Xu, J. Yang, C. Liu, H. Li, H. Zhou, L.H. Qu, Oridonin induces autophagy via inhibition of glucose metabolism in p53-mutated colorectal cancer cells, Cell Death Dis. 8 (2017) 2633.

[26] J. Zhou, E.J. Yun, W. Chen, Y. Ding, K. Wu, B. Wang, C. Ding, E. Hernandez, J. Santoyo, R.C. Pong, H. Chen, D. He, J. Zhou, J.T. Hsieh, Targeting 3-phosphoinositide-dependent protein kinase 1 associated with drug-resistant renal cell carcinoma using new oridonin analogs, Cell Death Dis. 8 (2017) 2701.

[27] K. Qing, Z. Jin, W. Fu, W. Wang, Z. Liu, X. Li, Z. Xu, J. Li, Synergistic effect of oridonin and a PI3K/mTOR inhibitor on the non-germinal center B cell-like subtype of diffuse large B cell lymphoma, J. Hematol. Oncol. 9 (2016) 72.

[28] K.E. Lazarski, B.J. Moritz, R.J. Thomson, The total synthesis of *Isodon* diterpenes, Angew. Chem. Int. Ed. 53 (2014) 10588-10599.

[29] A. Cernijenko, R. Risgaard, P.S. Baran, 11-Step total synthesis of (-)-Maoecrystal V, J. Am. Chem. Soc. 138 (2016) 9425-9428.

[30] J.T. Yeoman, V.W. Mak, S.E. Reisman, A unified strategy to *ent*-kauranoid natural products: total syntheses of (-)-trichorabdal A and (-)-longikaurin E, J. Am. Chem. Soc. 135 (2013) 11764-11767.

[31] J.Y. Cha, J.T. Yeoman, S.E. Reisman, A concise total synthesis of (-)-maoecrystal Z, J. Am. Chem. Soc. 133 (2011) 14964-14967.

[32] B.J. Moritz, D.J. Mack, L. Tong, R.J. Thomson, Total synthesis of the *Isodon* diterpene sculponeatin N, Angew. Chem. Int. Ed. 53 (2014) 2988-2991.

[33] L.M. Li, G.Y. Li, J.X. Pu, W.L. Xiao, L.S. Ding, H.D. Sun, *ent*-Kaurane and cembrane diterpenoids from *Isodon sculponeatus* and their cytotoxicity, J. Nat. Prod. 72 (2009) 1851-1856.

[34] W.G. Wang, B.C. Yan, X.N. Li, X. Du, H.Y. Wu, R. Zhan, Y. Li, J.X. Pu, H.D. Sun, 6,7-*Seco*-*ent*-kaurane-type diterpenoids from *Isodon eriocalyx* var. *laxiflora*, Tetrahedron 70 (2014) 7445-7453.

[35] H.D. Sun, S.X. Huang, Q.B. Han, Diterpenoids from *Isodon* species and their biological activities, Nat. Prod. Rep. 23 (2006) 673-698.

[36] M. Liu, W.G. Wang, H.D. Sun, J.X. Pu, Diterpenoids from *Isodon* species: an update, Nat. Prod. Rep. 34 (2017) 1090-1140.

[37] H. Li, R. Jiao, J. Mu, S. Xu, X. Li, X. Wang, Z. Li, J. Xu, H. Hua, D. Li, Bioactive natural spirolactone-type 6,7-*seco*-*ent*-kaurane diterpenoids and synthetic derivatives, Molecules 23 (2018) 2914.

[38] Z. Lv, B. Chen, C. Zhang, G. Liang, Total syntheses of trichorabdal A and maoecrystal Z, Chem. Eur. J. 24 (2018) 9773-9777.

[39] T.J. Maimone, P.S. Baran, Modern synthetic efforts toward biologically active terpenes, Nat. Chem. Biol. 3 (2007) 396-407.

[40] C. Tang, B. Wu, J. Wu, Z. Zhang, B. Yu, Novel strategies using total gastrodin and gastrodigenin, or total gastrodigenin for quality control of gastrodia elata, Molecules 23 (2018) 270.

[41] J. Wu, B. Wu, C. Tang, J. Zhao, Analytical techniques and pharmacokinetics of gastrodia elata blume and its constituents, Molecules 22 (2017) 1137.

[42] C. Tang, J. Wang, J. Yu, L. Wang, M. Cheng, W. Cui, J. Zhao, H. Xiao, Identification, characterization and in vitro neuroprotection of N^6-(4-hydroxybenzyl) adenine riboside and its metabolites, Phytochem. Lett. 20 (2017) 146-150.

[43] B. Meka, S.R. Ravada, M. Murali Krishna Kumar, K. Purna Nagasree, T. Golakoti, Synthesis of new analogs of AKBA and evaluation of their anti-inflammatory activities, Bioorg. Med. Chem. 25 (2017) 1374-1388.

[44] R. Cannalire, D. Machado, T. Felicetti, S. Santos Costa, S. Massari, G. Manfroni, M.L. Barreca, O. Tabarrini, I. Couto, M. Viveiros, S. Sabatini, V. Cecchetti, Natural isoflavone biochanin A as a template for the design of new and potent 3-phenylquinolone efflux inhibitors against mycobacterium avium, Eur. J. Med. Chem. 140 (2017) 321-330.

[45] G.G. Llanos, L.M. Araujo, I.A. Jimenez, L.M. Moujir, J. Rodriguez, C. Jimenez, I.L. Bazzocchi, Structure-based design, synthesis, and biological evaluation of withaferin A-analogues as potent apoptotic inducers, Eur. J. Med. Chem. 140 (2017) 52-64.

[46] J. Wang, R. Ge, X. Qiu, X. Xu, L. Wei, Z. Li, J. Bian, Discovery and synthesis of novel Wogonin derivatives with potent antitumor activity in vitro, Eur. J. Med. Chem. 140 (2017) 421-434.

[47] T. Han, J. Li, J. Xue, H. Li, F. Xu, K. Cheng, D. Li, Z. Li, M. Gao, H. Hua, Scutellarin derivatives as apoptosis inducers: Design, synthesis and biological evaluation, Eur. J. Med. Chem. 135 (2017) 270-281.

[48] B. Eignerova, M. Tichy, J. Krasulova, M. Kvasnica, L. Rarova, R. Christova, M. Urban, B.

Bednarczyk-Cwynar, M. Hajduch, J. Sarek, Synthesis and antiproliferative properties of new hydrophilic esters of triterpenic acids, Eur. J. Med. Chem. 140 (2017) 403-420.

[49] K. Tian, F. Xu, X. Gao, T. Han, J. Li, H. Pan, L. Zang, D. Li, Z. Li, T. Uchita, M. Gao, H. Hua, Nitric oxide-releasing derivatives of brefeldin A as potent and highly selective anticancer agents, Eur. J. Med. Chem. 136 (2017) 131-143.

[50] L. Wang, D. Li, S. Xu, H. Cai, H. Yao, Y. Zhang, J. Jiang, J. Xu, The conversion of oridonin to spirolactone-type or enmein-type diterpenoid: synthesis and biological evaluation of *ent*-6,7-*seco*-oridonin derivatives as novel potential anticancer agents, Eur. J. Med. Chem. 52 (2012) 242-250.

[51] D. Li, H. Cai, B. Jiang, G. Liu, Y. Wang, L. Wang, H. Yao, X. Wu, Y. Sun, J. Xu, Synthesis of spirolactone-type diterpenoid derivatives from kaurene-type oridonin with improved antiproliferative effects and their apoptosis-inducing activity in human hepatoma Bel-7402 cells, Eur. J. Med. Chem. 59 (2013) 322-328.

[52] D. Li, T. Han, K. Tian, S. Tang, S. Xu, X. Hu, L. Wang, Z. Li, H. Hua, J. Xu, Novel nitric oxide-releasing spirolactone-type diterpenoid derivatives with in vitro synergistic anticancer activity as apoptosis inducer, Bioorg. Med. Chem. Lett. 26 (2016) 4191-4196.

[53] S. Xu, H. Yao, M. Hu, D. Li, Z. Zhu, W. Xie, H. Yao, L. Wu, Z.S. Chen, J. Xu, 6,7-*Seco*-*ent*-kauranoids derived from oridonin as potential anticancer agents, J. Nat. Prod. 80 (2017) 2391-2398.

[54] A.K. Steiger, S. Pardue, C.G. Kevil, M.D. Pluth, Self-immolative thiocarbamates provide access to triggered H_2S donors and analyte replacement fluorescent probes, J. Am. Chem. Soc. 138 (2016) 7256-7259.

[55] G.K. Kolluru, X. Shen, S. Yuan, C.G. Kevil, Gasotransmitter heterocellular signaling, Antioxid. Redox Signal. 26 (2017) 936-960.

[56] J.L. Wallace, R. Wang, Hydrogen sulfide-based therapeutics: Exploiting a unique but ubiquitous gasotransmitter, Nat. Rev. Drug. Discov. 14 (2015) 329-345.

[57] C. Szabo, Gasotransmitters in cancer: From pathophysiology to experimental therapy, Nat. Rev. Drug. Discov. 15 (2016) 185-203.

[58] M. Whiteman, S. Le Trionnaire, M. Chopra, B. Fox, J. Whatmore, Emerging role of hydrogen sulfide in health and disease: Critical appraisal of biomarkers and pharmacological tools, Clin. Sci. 121

(2011) 459-488.

[59] D. Wu, J. Wang, H. Li, M. Xue, A. Ji, Y. Li, Role of hydrogen sulfide in ischemia-reperfusion injury, Oxid. Med. Cell Longev. 2015 (2015) 1-16.

[60] L. Xiao, J.H. Dong, X. Teng, S. Jin, H.M. Xue, S.Y. Liu, Q. Guo, W. Shen, X.C. Ni, Y.M. Wu, Hydrogen sulfide improves endothelial dysfunction in hypertension by activating peroxisome proliferator-activated receptor delta/endothelial nitric oxide synthase signaling, J. Hypertens. 36 (2018) 651-665.

[61] S. Mani, A. Untereiner, L. Wu, R. Wang, Hydrogen sulfide and the pathogenesis of atherosclerosis, Antioxid. Redox Signal. 20 (2014) 805-817.

[62] N. Sen, Functional and molecular insights of hydrogen sulfide signaling and protein sulfhydration, J. Mol. Biol. 429 (2017) 543-561.

[63] R.N. Carter, N.M. Morton, Cysteine and hydrogen sulphide in the regulation of metabolism: insights from genetics and pharmacology, J. Pathol. 238 (2016) 321-332.

[64] C. Szabo, A. Papapetropoulos, International union of basic and clinical pharmacology. CII: pharmacological modulation of H_2S Levels: H_2S donors and H_2S biosynthesis inhibitors, Pharmacol. Rev. 69 (2017) 497-564.

[65] Y.Y. Mok, M.S. Atan, C. Yoke Ping, W. Zhong Jing, M. Bhatia, S. Moochhala, P.K. Moore, Role of hydrogen sulphide in haemorrhagic shock in the rat: protective effect of inhibitors of hydrogen sulphide biosynthesis, Br. J. Pharmacol. 143 (2004) 881-889.

[66] D. Wu, M. Li, W. Tian, S. Wang, L. Cui, H. Li, H. Wang, A. Ji, Y. Li, Hydrogen sulfide acts as a double-edged sword in human hepatocellular carcinoma cells through EGFR/ERK/MMP-2 and PTEN/AKT signaling pathways, Sci. Rep. 7 (2017) 5134.

[67] S.S. Wang, Y.H. Chen, N. Chen, L.J. Wang, D.X. Chen, H.L. Weng, S. Dooley, H.G. Ding, Hydrogen sulfide promotes autophagy of hepatocellular carcinoma cells through the PI3K/Akt/mTOR signaling pathway, Cell Death Dis. 8 (2017) 2688.

[68] J.L. Wallace, J.G. Ferraz, M.N. Muscara, Hydrogen sulfide: an endogenous mediator of resolution of inflammation and injury, Antioxid. Redox Signal. 17 (2012) 58-67.

[69] Y. Zhen, W. Zhang, C. Liu, J. He, Y. Lu, R. Guo, J. Feng, Y. Zhang, J. Chen, Exogenous hydrogen sulfide promotes C6 glioma cell growth through activation of the p38 MAPK/ERK1/2-COX-2 pathways, Oncol. Rep. 34 (2015) 2413-2422.

[70] K. Kashfi, Anti-cancer activity of new designer hydrogen sulfide-donating hybrids, Antioxid. Redox Signal. 20 (2014) 831-846.

[71] X. Hu, R. Jiao, H. Li, X. Wang, H. Lyu, X. Gao, F. Xu, Z. Li, H. Hua, D. Li, Antiproliferative hydrogen sulfide releasing evodiamine derivatives and their apoptosis inducing properties, Eur. J. Med. Chem. 151 (2018) 376-388.

[72] M. Li, J. Li, T. Zhang, Q. Zhao, J. Cheng, B. Liu, Z. Wang, L. Zhao, C. Wang, Syntheses, toxicities and anti-inflammation of H_2S-donors based on non-steroidal anti-inflammatory drugs, Eur. J. Med. Chem. 138 (2017) 51-65.

[73] L. Li, M. Whiteman, Y.Y. Guan, K.L. Neo, Y. Cheng, S.W. Lee, Y. Zhao, R. Baskar, C.H. Tan, P.K. Moore, Characterization of a novel, water-soluble hydrogen sulfide-releasing molecule (GYY4137): New insights into the biology of hydrogen sulfide, Circulation 117 (2008) 2351-2360.

[74] J. Kang, A.J. Ferrell, W. Chen, D. Wang, M. Xian, Cyclic acyl disulfides and acyl selenylsulfides as the precursors for persulfides (RSSH), selenylsulfides (RSeSH), and hydrogen sulfide (H_2S), Org. Lett. 20 (2018) 852-855.

[75] J.L. Wallace, G. Caliendo, V. Santagada, G. Cirino, Markedly reduced toxicity of a hydrogen sulphide-releasing derivative of naproxen (ATB-346), Br. J. Pharmacol. 159 (2010) 1236-1246.

[76] M. Chattopadhyay, R. Kodela, K.R. Olson, K. Kashfi, NOSH-aspirin (NBS-1120), a novel nitric oxide- and hydrogen sulfide-releasing hybrid is a potent inhibitor of colon cancer cell growth in vitro and in a xenograft mouse model, Biochem. Biophys. Res. Commun. 419 (2012) 523-528.

[77] J.W. Elrod, J.W. Calvert, J. Morrison, J.E. Doeller, D.W. Kraus, L. Tao, X. Jiao, R. Scalia, L. Kiss, C. Szabo, H. Kimura, C.W. Chow, D.J. Lefer, Hydrogen sulfide attenuates myocardial ischemia-reperfusion injury by preservation of mitochondrial function, Proc. Natl. Acad. Sci. U. S. A 104 (2007) 15560-15565.

[78] B. Szczesny, K. Modis, K. Yanagi, C. Coletta, S. Le Trionnaire, A. Perry, M.E. Wood, M. Whiteman, C. Szabo, AP39, a novel mitochondria-targeted hydrogen sulfide donor, stimulates cellular bioenergetics, exerts cytoprotective effects and protects against the loss of mitochondrial DNA integrity in oxidatively stressed endothelial cells in vitro, Nitric oxide 41 (2014) 120-130.

[79] J.M. Paquette, M. Rufiange, M. Iovu Niculita, J. Massicotte, M. Lefebvre, P. Colin, A. Telmat, M. Ranger, Safety, tolerability and pharmacokinetics of trimebutine 3-thiocarbamoylbenzenesulfonate (GIC-1001) in a randomized phase I integrated design study: single and multiple ascending doses and

effect of food in healthy volunteers, Clin. Ther. 36 (2014) 1650-1664.

[80] P. Qiu, S. Zhang, Y. Zhou, M. Zhu, Y. Kang, D. Chen, J. Wang, P. Zhou, W. Li, Q. Xu, R. Jin, J. Wu, G. Liang, Synthesis and evaluation of asymmetric curcuminoid analogs as potential anticancer agents that downregulate NF-kB activation and enhance the sensitivity of gastric cancer cell lines to irinotecan chemotherapy, Eur. J. Med. Chem. 139 (2017) 917-925.

[81] S. Ma, D. Zhong, P. Ma, G. Li, W. Hua, Y. Sun, N. Liu, L. Zhang, W. Zhang, Exogenous Hydrogen Sulfide Ameliorates Diabetes-Associated Cognitive Decline by Regulating the Mitochondria-Mediated Apoptotic Pathway and IL-23/IL-17 Expression in db/db Mice, Cell Physiol. Biochem. 41 (2017) 1838-1850.

[82] F. Xu, X. Gao, H. Li, S. Xu, X. Li, X. Hu, Z. Li, J. Xu, H. Hua, D. Li, Hydrogen sulfide releasing enmein-type diterpenoid derivatives as apoptosis inducers through mitochondria-related pathways, Bioorg. Chem. 82 (2018) 192-203.

[83] Z. Bai, J. Zhang, Q. Zhang, T. Zhang, J. Li, Q. Zhao, Z. Wang, D. He, J. Cheng, J. Zhang, B. Liu, Synthesis, toxicities and bio-activities of manganese complexes with CO and H_2S dual donors, Eur. J. Med. Chem. 159 (2018) 339-356.

[84] X. Gao, J. Li, M. Wang, S. Xu, W. Liu, L. Zang, Z. Li, H. Hua, J. Xu, D. Li, Novel enmein-type diterpenoid hybrids coupled with nitrogen mustards: Synthesis of promising candidates for anticancer therapeutics, Eur. J. Med. Chem. 146 (2018) 588-598.

[85] T. Han, K. Tian, H. Pan, Y. Liu, F. Xu, Z. Li, T. Uchita, M. Gao, H. Hua, D. Li, Novel hybrids of brefeldin A and nitrogen mustards with improved antiproliferative selectivity: Design, synthesis and antitumor biological evaluation, Eur. J. Med. Chem. 150 (2018) 53-63.

Highlights

- H_2S donating *ent*-kaurane and spirolactone-type derivatives were synthesized.
- **12b** showed potent antiproliferative effect against Bel-7402 cells.
- **12b** arrested Bel-7402 cell cycle at G_1 phase and induced mitochondria dysfunction.
- **12b** regulated the expression of apoptosis-related proteins.